HOST UNIVERSITY: The University of Queensland

FACULTY: Engineering, Architecture and Information Technology

DEPARTMENT: School of Civil Engineering

Academic Year 2015-2016

STUDY ON THE EFFECTIVENESS OF SPRINKLERS IN TUNNELS

Daan Van den Broecke

Promoters:

Prof. Bart Merci

Prof. José L. Torero

Dr. Cristian Maluk

Master thesis submitted in the Erasmus Mundus Study Programme

International Master of Science in Fire Safety Engineering

This page is intentionally left blank.

Declaration

This thesis is submitted in partial fulfillment of the requirements for the degree of *The International Master of Science in Fire Safety Engineering (IMFSE)*. This thesis has never been submitted for any degree or examination to any other University/programme. The author(s) declare(s) that this thesis is original work except where stated. This declaration constitutes an assertion that full and accurate references and citations have been included for all material, directly included and indirectly contributing to the thesis. The author(s) gives (give) permission to make this master thesis available for consultation and to copy parts of this master thesis for personal use. In the case of any other use, the limitations of the copyright have to be respected, in particular with regard to the obligation to state expressly the source when quoting results from this master thesis. The thesis supervisor must be informed when data or results are used.

April 30, 2016

Read and approved

Abstract

In this thesis the effectiveness of a deluge sprinkler system on car fires was studied by performing a series of full-scale experiments.

The required water flow for deluge systems in tunnels is currently not prescribed in most parts of the world. It is currently unclear above which water flow the deluge system suppresses a car fire and below which it fails to do so. This thesis aims at bridging this gap in tunnel fire suppression knowledge.

Full-scale car fire experiments with a deluge nozzle at 5.5 m height were carried out. Various water flows were tested for the deluge system and its influence on the temperatures around and above the car was quantified. The influence the deluge system had on the fire was investigated with IR camera footage and thermocouples.

It was found that there are two main forms of suppression; gradual and instantaneous. Extinction of car fires by deluge systems is shown to be an improper term since the seat of the fire cannot be reached. It was found that a water flow of 6.6 mm/min can drop the temperatures in the immediate vicinity of the car. A relationship between the heat release rate of a fire and the required water flow for the deluge system is presented.

Abstract

In deze thesis wordt het effect van een deluge sprinklerinstallatie op een brandende auto onderzocht door middel van een reeks experimenten op ware grootte.

De benodigde waterstroom voor deluge systemen in tunnels wordt momenteel niet voorgeschreven in de meeste delen van de wereld. Het is op dit moment onduidelijk boven welke hoeveelheid water het deluge systeem een autobrand kan bestrijden en voor welke hoeveelheid het systeem faalt. Deze thesis is gericht op het overbruggen van de huidige leemte in kennis omtrent actieve brandblusinstallaties in tunnels.

De experimenten werden uitgevoerd op ware grootte met een deluge sprinklerkop op 5.5 m hoogte. Verscheidene waterstromen werden getest en de invloed op temperaturen rondom en boven een brandende auto werd onderzocht. Het effect van het deluge sprinklersysteem werd geanalyseerd met behulp van een infrarood camera en thermokoppels.

Uit het experimentele onderzoek is gebleken dat er hoofdzakelijk twee vormen van brandbestrijding ten gevolge van het deluge systeem kunnen zijn: geleidelijke en onmiddellijke brandonderdrukking. Het blussen van een autobrand bleek geen gepaste term voor deluge systemen in tunnels, aangezien de brandhaard zelf niet kan worden bereikt. Er werd gevonden dat een capaciteit van 6.6 mm/min voldoende kan zijn om de temperatuur in de directe nabijheid van de auto te koelen. Een relatie tussen het brandvermogen en het waterdebiet wordt gepresenteerd.

Acknowledgements

I would like to thank Dr. Cristián Maluk Zedan for his constant feedback and availability. His input was crucial at any stage of my thesis.

I would like to thank both of my promoters Prof. Bart Merci and Prof. Jose L. Torero. Not only for their guidance during the various stages of the thesis, but also for their invaluable efforts to making the IMFSE program what it is today.

A big thanks goes out to Toni Sietz and Michael Conway from QFES. Toni's design of the steel frame was simply brilliant and the help from people at QFES was exceptional.

Thanks to Nick Agnew from StaceyAgnew for giving me an introduction on tunnel fire safety and letting me use the deluge nozzles.

Thank you to Jeronimo Carrascal Tirado for helping me sort out the lab equipment and to the entire fire team for helping out with the experiment.

Lastly, on a more personal note, I would like to thank some people in their mother tongue:

Obrigado pelo apoio durante toda a minha tese, Julia.

Ik zou graag mijn ouders bedanken voor de kansen die mij gegeven zijn en mijn oudere broer, voor de voorbeeldfiguur die hij is en altijd zal zijn.

Helaas kan mijn grootmoeder het niet meer meemaken dat ik deze studies afrond. Ik zou graag dit werk opdragen aan haar.

Contents

List of Figures

List of Tables

Chapter 1

Introduction

1.1 Background

Increasing urbanisation and population growth drives a need for more efficient transportation solutions. In the past decades the world has become more connected through means of communication and mobility. At the same time, environmental and geographical constraints challenge the way transportation evolves. As a way to overcome these hurdles in an efficient manner tunnels are becoming more present in modern infrastructure developments.

The efficient and elegant mobility solution of a tunnel has numerous fire safety concerns that should be addressed. It is a very specific enclosure that demands tailored fire safety systems. The problem here is that some fundamental research for tunnel fires is still to be done in order to fully understand its fire dynamics.

Deluge sprinkler systems, characterised by large water flows and big droplet sizes, are the most common Fixed Fire Fighting System (FFFS) for tunnels; however, there seems to be no general consensus on their application in tunnels. First, because of the big cost associated with installation, maintenance and drainage of these systems. Second, because the required water flow rate to suppress a tunnel fire remains unclear; there is a lack of experimental research in this field and the definition of a suppression system allows for interpretation.

Currently, there are two countries that put deluge systems in their tunnels as a general rule: Japan and Australia. Japan prescribes a water flow of 6 mm/min whereas the Australian requirement is 10 mm/min. The substantial difference between these requirements express the uncertainty of underlying fire science. In countries where there is a lack of prescriptive framework regarding deluge systems in tunnels, often, a more conservative water flow is applied.

1.2 Aim of Research

The work presented in this thesis intends to contribute to fundamental tunnel fire suppression knowledge. The experiments described further are carried out by varying water flows for a deluge sprinkler system on a car fire. The influence of various water flows on different car fire sizes is assessed. In order to justify the cost associated with tunnel deluge systems, an efficient suppression system is paramount. The ultimate objective for this work would be to optimise deluge systems.

1.3 Outline of Chapters

The work described herein is presented in 6 chapters. The chapter following this introduction presents a thorough literature review about the fire dynamics and the use of suppression systems in tunnels. It also presents the current knowledge on the required water flow to suppress different kinds of fire. This chapter defines the backbone and the need for the work presented in this thesis.

The subsequent chapter describes the methodology. It is explained how the experimental research is carried out and goes through the various steps of the process.

In the results section of this thesis, the experimental outcomes are shown. This section summarises the data extracted from the experiments and is discusses upon in the subsequent discussion section.

The final chapter of this thesis lists the conclusions; here the main findings of this work are presented, with a discussion of future research needed in the field of FFFS in tunnels.

Chapter 2

Literature Review

2.1 Tunnel Fires

Due to the distinct ventilation and fuel load conditions, tunnel fires pose a unique fire behaviour. Not only are tunnel fires more likely to be shielded, there is also shielding from the tunnel structure itself; providing the fire with additional thermal feedback from the tunnel linings.

Prior experimental research [7] has shown that ventilation in tunnels is a driving factor for fire growth rate and fire severity. It is worth highlighting that a tunnel fire can both be ventilation controlled or fuel controlled, although in most cases, the latter situation will occur [22]. On one hand, keeping ventilation to a strict minimum would keep the fire from growing very rapidly to extreme heat releases. On the other hand, ventilation is required to prevent back-layering and provide tenable egress conditions upstream from the tunnel. A controversial question regarding this ventilation tradeoff is put forward by Carvel [7]: *'Which is worse, back-layering or rapid fire growth?*. The answer to this seemingly simple question is quite complex and lies in finding the right compromise.

A typical approach in enclosure fire dynamics is the assumption of a t^2 growth rate before reaching a ventilation-controlled maximum fire size. However, a two-step linear growth model [7] has shown to be more appropriate to describe tunnel fire dynamics. The first step in this model is the 'incubation' phase, which can be anywhere in between just a few minutes to several tens of minutes [28]. This step is followed by a rapid growth phase that typically

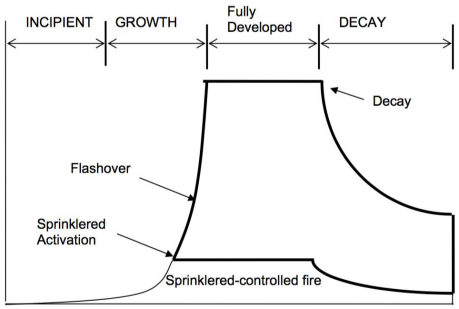

Figure 2.1: Schematic of a tunnel design fire scenario [15]

reaches the maximum fire size in a few minutes and often lasts less than 10 minutes. Figure 2.1 shows a schematic of a tunnel design fire, including the supposed effect of using an active suppression system.

Design fires for structural elements are often expressed as time-temperature curves. These design fires differ from country to country and even within a body such as the European union, design fires vary. Furthermore, the performance criteria when designing fire safe structural behaviour of tunnels vary across different jurisdictions.

France defines four fire resistance levels: N0 to N3 [15]. N0 is the least strict resistance level and corresponds with the situation where there is no risk of progressive collapse in case of a local failure. Any structure must satisfy this requirement. Level N1 corresponds to a resistance of 120 minutes to the well-known ISO curve (See figure 2.2). This ensures structural resistance to all but the most violent fires [15]. Level N2 corresponds to resistance to the increased hydrocarbon curve (see HC increased curve in figure 2.2. The strictest fire resistance level, N3, corresponds with a resistance to the ISO curve during 240 minutes and the increased hydrocarbon curve during 120 minutes. In order to satisfy both curves must be tested separately.

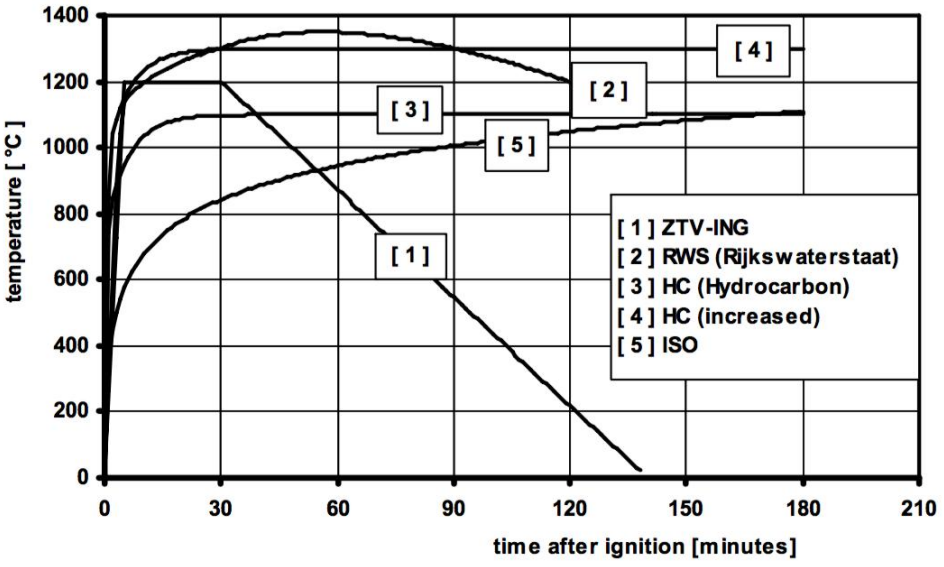

Figure 2.2: Tunnel design fire temperature curves [15]

The ZTV-ING curve in figure 2.2 shows the design fire temperature curve used in Germany. The ZTV-ING prescribes that temperatures cannot exceed 300 °C at the reinforcement of the tunnel as a consequence of the design

fire [15]. Germany uses the ISO curve when referring to the escape door fire resistance (90 min).

In the Netherlands, the RWS curve (Figure 2.2) is used as a reference [15]. This curve is amongst the strictest and is linked with the fact that there are many underwater tunnels in the Netherlands. Therefore a very strict requirement is set out regarding water tightness and collapse. Temperature-wise, the requirements tell that when subjected to the RWS curve for two hours (and extended with an extra hour), the heat resistance of the lining should comply with the following: $\leqslant 380°C$ at the lining-concrete interface; $\leqslant 250°C$ for the steel reinforcement mesh and $\leqslant 60°C$ at any present rubber joint gasket.

The latest PIARC objectives [34] require resistance to the ISO curve for 60 minutes for the main structural elements if the traffic type can be defined as cars and vans. For the case of trucks and tankers resistance to the RWS or increased HC curve is required during 120 min. Tunnels with a very heavy traffic of trucks with combustible goods may have a requirement of 180 min.

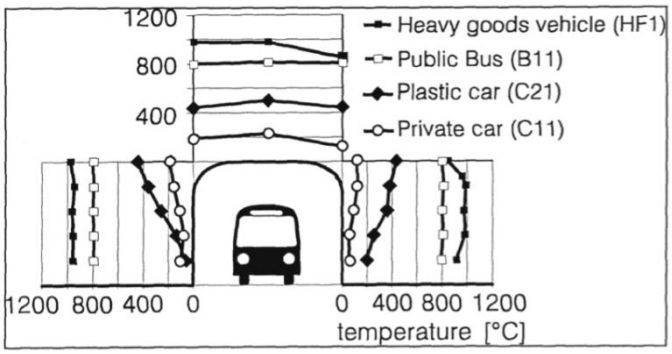

Figure 2.3: Tunnel interface temperatures for different cars (EUREKA) [15]

PIARC issued a report [10] in 1987 with maximum temperatures at the tunnel wall during different kind of vehicle fires. The temperature values given were 400°C for a passenger car, 700°C for a bus or truck and 1000°C for a petrol tanker. For these experiments there was a minimal longitudinal air flow to prevent back-layering and the measurement was taken 10 m in the direction of the airflow. These temperatures were roughly confirmed by the EUREKA tests [1] although for the passenger car a higher temperature of 500°C was measured. The maximum temperatures of the tunnel linings during road vehicle tests are shown in figure 2.3 [15]. This figure shows the maximum temperature distributions for four different vehicle sizes.

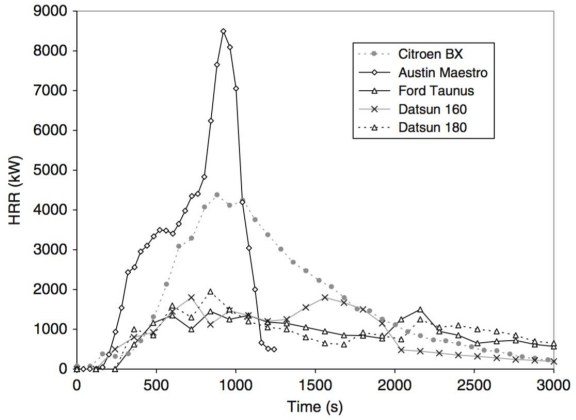

(a) HRR of cars tested at FRS [42] and VTT [29]

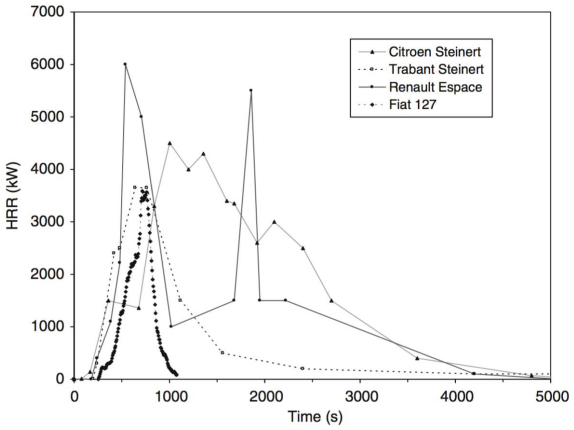

(b) HRR of cars tested at MFPA [44] and SP [23]

Figure 2.4: Overview of car fire HRR-curves [3]

2.1.1 Fire Dynamics

The Ford Taunus, the Datsun 160J and the Datsun 180B from figure 2.4a were tested by VTT in Finland and have a peak HRR of 1.5 MW, 1.7 MW and 1.8 MW respectively [29]. The Citroën BX and Austin Maestro data in this figure originates from similar tests performed by Shipp and Spearpoint [42] at the Fire Research Station (FRS). Amongst these test results there appears to be one outlier, the Austin Maestro, that went up 8.5 MW. Apart from this curve the results appear to be consistent with peak HRRs in the order of 2.0-4.5 MW.

Figure 2.4b shows the HRR curves of four more cars. MFPA [44] tested a Citroën, a Trabant and a Renault Espace. The Fiat 127 test results come from SP Technical Research Institute of Sweden [23]. The peak HRR of these cars was found around 3.5-6 MW. For the Renault there are two peaks in

the HRR curve, this could be explained by additional fuel load -such as the tires- becoming involved in the fire. Another explanation could be that more fuel gets involved in the fire following failure of the fire barrier.

PIARC [34], the French guidelines [25] and NFPA [32] define the HRR for a big passenger car to be 5 MW. PIARC and the French guideline also define a light passenger car to be 2.5 MW. All three of these guidelines set the HRR of two to three passenger cars at 8 MW.

A summary of the time that it takes to reach the peak HRR and its magnitude is given in figure 2.5. After dividing this figure into 5 MW intervals, it becomes clear that the majority of single car fires burn with a peak HRR of less than 5 MW. Two-car fires are located in the 5 to 10 MW interval whereas the three-car fires can burn with a peak HRR of just over 15 MW.

There is a linear tendency of peak HRR with increasing total caloric content of a passenger [15]. Additionally, a recent study has shown that the caloric content of passenger cars has been increasing throughout the past decades [24]. This must be taken into account when using experimental data to determine the design fire. Another important factor is the traffic intensity as this is directly related to the amount of cars potentially involved and the spacing between vehicles.

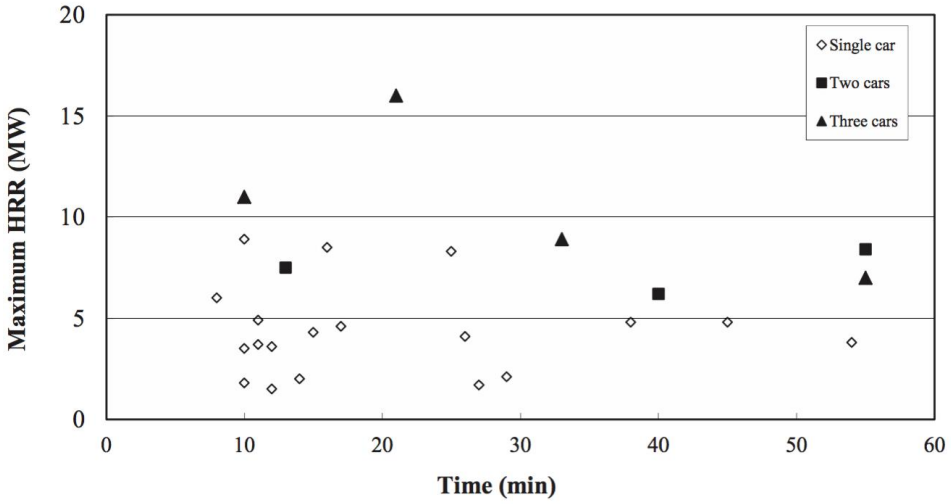

Figure 2.5: Maximum HHR values for passenger cars [22]

Making sure the fire stays contained to the initially involved vehicle(s) is one of the main the objectives of a FFFS (see 2.2). In order to design these systems, the mechanisms by which fire spreads from one car onto the

next needs to be properly understood. A model used in the Channel tunnel assessments [38] identified the main mechanisms of fire spread in tunnel fires [22]:

1. Flame impingement: flames 'crawling' along the tunnel ceiling above downstream vehicles.
2. Flame spread across a surface: the flame spreading by pyrolysing adjacent materials.
3. Remote ignition by radiation: radiation from a burning vehicle igniting vehicles in the direct proximity. Research has shown that the radiated fraction of the total heat release is about 30% [30].
4. Fuel transfer: this includes both spread by burning liquid and fire being transported downstream from the fire. The fuel spread direction is typically downhill for liquids and downwind for firebrands.
5. Explosion: there are potentially explosive components present in vehicles such as the tires, airbags and the fuel tank.

Given the fact that many tunnel fires are the consequence of a collision (See table 2.1 and, additional fuel is likely to be close to the fire source; the most plausible flame spread mechanisms that explain fire spread to multiple vehicles are flame impingement and remote or spontaneous ignition by radiation [9]. It is estimated that approximately 4 to 5 fires occur for every 100 million vehicle km [5]. This estimate is based on European statistics and shows that less than 1% of the fires have serious consequences. A majority of those serious cases is the result of an accident. Another cause is self-ignition of a heavy goods vehicle. The latter occurred in the Mont Blanc tunnel fire but is generally seen as uncommon.

2.1.2 Duration of the Fire

The duration of recorded (serious) tunnel fires in the last decades ranges from 20 minutes to 4 days, with typical durations in the order of 2-3 hours [12]. The outlier, with an exceptionally long duration of 4 days, was the Nihonzaka Tunnel Fire (Japan) in 1979. This tunnel fire was caused by the collision between four trucks and two small passenger cars. The fire then spread to an additional 173 cars located upstream from the collision. Other examples of particularly serious tunnel fires include the Mont Blanc tunnel (France/Italy) and the Tauern (Austria) Tunnel, both in 1999. Those tunnel fires lasted for 53 and 15 hours, respectively. The tunnel fire in the Gotthard Tunnel (Switzerland) of 2001 had a duration of 20 hours. Table 2.1 gives more information on the vehicles that were involved in these tunnel fires.

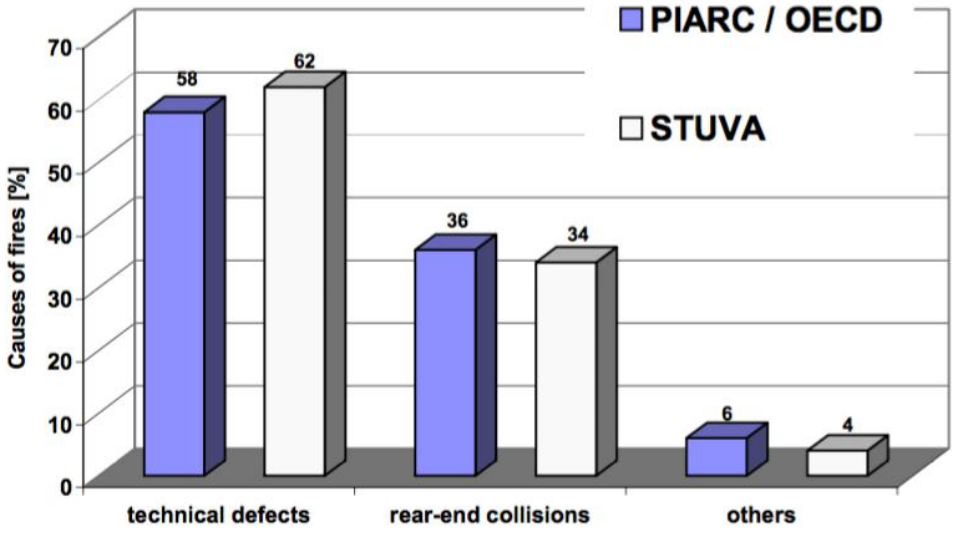

Figure 2.6: Causes of vehicle fires in road tunnels according to analysis of PIARC/OECD and STUVA [16]

2.2 Sprinklers in Tunnels

The terminology on suppression and, more broadly, water-based suppression systems can be somewhat misleading [8]. In essence, a suppression system does not necessarily suppress the fire although it attempts to do so. Similarly, a fixed firefighting system does not necessarily have the ability to 'fight' the fire. The ability for deluge systems in tunnels to suppress or fight the fire is not guaranteed, however, the ability to protect the tunnel structure has been well documented [43]. Since tunneling projects involve many parties, it is essential that there is a consensus on a clear suppression definition. Note that suppression is often not the failure/success story, but has a grey zone and should therefore be assessed in a more quantifiable method.

The main difference between the different sprinkler systems lies in the sprinkler nozzles and consequently the pressure of the system. In general, sprinkler systems can be divided in three categories:

- Conventional sprinkler systems
- Deluge sprinkler systems
- Water mist systems

Conventional sprinkler heads are usually equipped with a bulb that breaks at a certain temperature. In a wet pipe system, the water can leave the

sprinkler after breakage of this bulb. In the dry pipe case, another valve has to be opened after breakage to allow for the water to flow. This is applied in cases where accidental sprinkler head activation could is likely to occur or where the nature of stored goods steers towards extra caution.

Deluge sprinkler heads have open nozzles, meaning that they do not have heat sensitive bulbs. They are dry pipe systems and most commonly have a two-step activation. First a detection device would warn a central unit and secondly the system would be manually activated, usually after the fire has been located and identified at a central control unit. The working principle of this system is to flood the affected section with big droplets; effectively removing heat, cooling surfaces and consequently inhibiting the combustion process [36]. The application rate for this type of sprinklers is typically given in mm/min (or $l/min/m^2$) rather than droplet size distribution [36]. The big deluge droplets (in the order of 1 mm [9]) have the mass and momentum to penetrate to the seat of the fire. However, as is the case with a car fire, the seat of the fire is not always easily accessible.

The third type of sprinklers is water mist systems. These systems have a whole different suppression strategy. The droplets in these systems are very small (50-250 µm [9]) and can effectively cool the environment in which they are deployed. In order to generate these small droplets, the system operates under high pressures. Because of the small scale of the droplets, they can interact on a flame-level and reduce the fire size. However, unlike deluge systems, they do not succeed in penetrating, wetting and attacking the seat of the fire. Given the longitudinal airflows in tunnels, water mist droplets are very likely to be heavily deflected and hence their application in tunnels is quite controversial. It is shown in figure 2.7 of the following section that water mist droplets can deflect significantly.

2.2.1 Historical Background

An overview of recent tunnel fires with multiple vehicles involved is given in table 2.1.
Interestingly, the use of sprinklers in tunnels is a very controversial topic despite big tunnel fires occurring on a yearly basis (see table 2.1). The World Road Association, PIARC, advised against the use of sprinklers in tunnels in their 1999 report on "Fire and Smoke Control in Road Tunnels" [34]. It stated that the use of sprinklers could be problematic because:

- Water can cause explosion in petrol and other chemical substances if not combined with appropriate additives;
- There is a risk that the fire is extinguished but flammable gases are still produced and may cause an explosion;

Table 2.1: Overview of recent tunnel fires with multiple vehicles [20]

Tunnel	Cause	Vehicles involved	Country	Year
Eiksund Tunnel	Collision	Lorry and van	Norway	2009
Channel Tunnel	Possible electrical fire	25 HGV and 2 vans, train locomotive and carriages	UK/France	2008
Newhall Pass Tunnel	Collision	33 HGV	USA	2007
Burnley Tunnel	Collision	3 HGV and 4 cars	Australia	2007
Viamala Tunnel	Collision	Bus and 2 cars	Switzerland	2006
Fréjus Tunnel	Overheating	4 HGV	France/Italy	2005
Baregg Tunnel	Collision	3 HGV and car	Switzerland	2004
Daegu Subway	Arson	2 subway trains	South Korea	2003
St Gotthard Tunnel	Collision	23 vehicles, most HGV	Switzerland	2001
Tauern Tunnel	Collision	16 HGV and 24 cars	Austria	1999
Mont Blanc Tunnel	Overheating	34 vehicles, most HGV	France/Italy	1999
Channel Tunnel	Possible overheating	10 HGV, train locomotive and carriages	UK/France	1996

- Vaporised steam can hurt people;
- The efficiency is low for fires inside vehicles;
- The smoke layer is cooled down and de-stratified, so that it may cover the whole tunnel;
- Maintenance can be costly;
- Sprinklers are difficult to handle manually; and
- Visibility is reduced.

Because of the aforementioned reasons, it was believed that a sprinkler system could cause harm to people and could therefore not fulfil the purpose of a life safety system. It was concluded that, because of the potential risks, sprinkler systems could only be used after evacuation of the tunnel [46]. PIARC issued a document in 2008 that carefully acknowledged the potential of FFFS [35]. It stated that *In most cases, FFFS are not capable of extinguishing vehicle fires. The aims are to: slow down fire development, reduce or completely prevent fire from spreading to other vehicles, provide for safe evacuation, maintain tenability for fire-fighting operations, protect the tunnel structure and limit environmental pollution.* Amongst other things, it is added that these systems should be designed to handle air velocities of 10 m/s. Research [14] carried out at the BRE Centre for Fire Safety Engineering in the UK underlines that handling 10 m/s is not feasible as design criteria. Their research showed that even droplets in the order of 300 µm, or simply coalesced droplets from a typical sprinkler system, can undergo a displacement in the order of 40-50 m for given longitudinal air flow (see figure 2.7). The 10 m/s statement, as expressed by the World Road Association in the 2008 report, emphasises the need for further experimental research in tunnel suppression systems following this report.

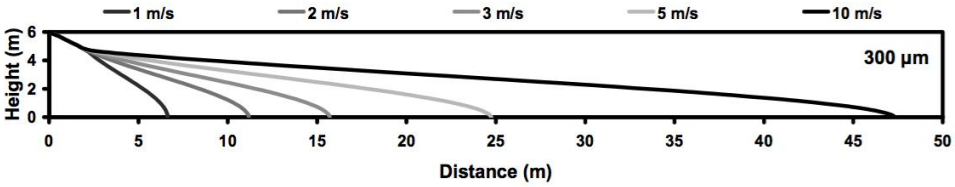

Figure 2.7: Travelling distances for 300 µm droplets in a horizontal tunnel section, subject to varying longitudinal air flows [14]

Similarly to what happened after the 1999 report of PIARC, further research has been carried out after issuing the 2008 report. These research programs further changed the mind-set in favour of FFFS. The latest 2016 report [36] states that FFFS allow:

- fires to be addressed in a timely manner before the fire brigade arrives
- delivery of sufficient water to the fire site, such that control or suppression of a fire can occur before the fire develops into a full scale conflagration
- the fire brigade to manage the fire incident without putting themselves at risk by being in the near vicinity of a fire
- the fire brigade to fully extinguish the fire once it has been suppressed (if it has not already been extinguished)

Note that the 2008 report of PIARC stated that there could not be extinguishment for vehicle fires in tunnels and that the last bullet point of the 2016 advantages mentions potential extinguishment.

The Fire in Tunnels Network (FIT) in Europe gives an overview [15] of the advantages and disadvantages for sprinklers in tunnels. The advantages are:

- It will be able to limit a beginning fire before arrival of the fire brigade
- It will facilitate easier access to the fire because of lowered temperatures
- It will slow down the fire development and lower fire size and duration
- Damage can be limited by creating less harsh conditions in the tunnel. A sprinkler system will generally use less water than a fire department to extinguish the fire

The advantages all come down the last bullet point; creating less harsh conditions in the tunnel. The statement that a sprinkler system uses less water than the fire brigade is, certainly for the deluge sprinkler case, arguable. The report [15] continues with listing some disadvantages:

- A wet sprinkler system could be activated by accident
- The sprinkler will cool down the smoke and prevent stratification. This will mix the air with the smoke and prevent escape
- Visibility is limited because of steam
- Sprinklers will not serve its purpose to limit the size of a small fire since it can only fight the fire that is outside of the car and by then the fire would be fully developed
- Evacuation (drainage) of the water needs to be treated
- Sprinklers break down when subjected to a certain amount of heat. Therefore they will not have an effect on dangerous good fires that immediately develop to large fires.

The report concludes with stating: *If escape routes and lights are available that allow rapid escape of persons inside a tunnel, a well-serviced and accurate sprinkler system can be a good way of limiting damage done to the structure of the tunnel for some -but not all- types of fire* [15]. It is worth noting that the European Directive (2004) [11] on minimum safety requirements for road tunnels does not mention FFFS.

Note that the FIT, similarly to PIARC in the early 2000s, is very careful in recommending sprinklers in tunnels and emphasises the possibly disadvantages. A technical report (2006) [19] from the Fire in Tunnels Network, giving an overview of the fire suppression guidelines in Europe, states that *Sprinklers are generally not mentioned or discouraged.* The BD78/99 guideline in the UK declares that FFFS are not considered suitable for traffic space [15]. The NL-safe guideline in the Netherlands acknowledges that sprinklers can be used for mitigating the heating of concrete and reinforcement [15]. It is no common practice to put sprinklers in tunnels in the Netherlands although a change in mentality appears to have occurred with the Benelux II and the Betuwelijn Tunnel.

The 2014 edition of NFPA 502 [32] states in its appendix E that FFFS in tunnels are widely recognised by fire fighters and can be effective for fire control by limiting fire spread. It is noted that FFFS can be a valuable component of the overall fire safety system in a tunnel. NFPA 502 recommends an activation time of maximum three minutes in order to prevent a major, unmanageable fire. A Swedish research [27] suggested a fire that grows beyond 25 MW would become difficult to fight. In order keep fire sizes manageable it suggests the installation of FFFS.

Japan has by far the most experience with deluge systems. In the fifty years they have been deploying sprinklers in their tunnels, deluge activation

Table 2.2: Absolute minimum water requirements for extinguishment [21]

Vehicle	Fire area [m2]	HRR [MW]	Water required for extinguishment [l/min]	No. of 360 l/min jets
Passenger car	10	5	226	1
Van	35	15	462	2
Truck	200	100	1250	4

occurred in 16 instances. None of these fires escalated to disastrous proportions and the Japanese tunnel authorities have been found satisfied with the sprinkler performance [45]. Experience in Australia is more scarce, they have been deploying sprinklers in tunnels since 1992 in the Sydney Harbour Tunnel. In 2007, the deluge system of the Burnley Tunnel in Melbourne was proven to be successful during a fire [9].

2.2.2 Required Water Flow

Water is an extraordinary efficient medium to attack a fire. Given the small molecule size, water should never have the capability to absorb heat the way it does. The hydrogen bonds allow water to have a latent heat of up to 2458 kJ/kg. In other words, in order for 1kg of water to evaporate, approximately 2.5 MJ of energy is absorbed [8]. This gives an idea of water's suppressing capacity; if we manage to release 1 litre of water per second on a 2.5 MW fire, the water will absorb all the heat from the fire. However, in reality the story is more complex. The extent to which the water evaporates is strongly dependent on the droplet size. This could lead to the premature conclusion of rating water mist as the number one fixed fire fighting since its droplets will evaporate more easily. Again, reality is more complex. Water mist droplets will not reach the seat of the fire and will therefore not attack the fire source or actively cool/wet the surfaces in the direct vicinity of the fire the way a deluge system would.

Table 2.2 gives the minimum water requirement fire-fighters need to extinguish a vehicle fire. These estimates are based on the requirements for non-residential buildings and assume straightforward access to the fire [39]. Since vehicle fires are typically difficult to reach, these values should be treated as order of magnitude estimates of the absolute minimum water requirement. Note that a fire-fighter has a far greater efficiency than a sprinkler system.

The required sprinkler water flow for tunnels is prescribed by legislation in Japan and Australia. Japan requires a water flow of 6 mm/min [45] whereas Australia demands a 10 mm/min [4] water flow. The Benelux II tunnel in the Netherlands deploys 12 mm/min for its deluge system. These values

are plotted in figure 2.8 on top of the required water densities according to NFPA 13.

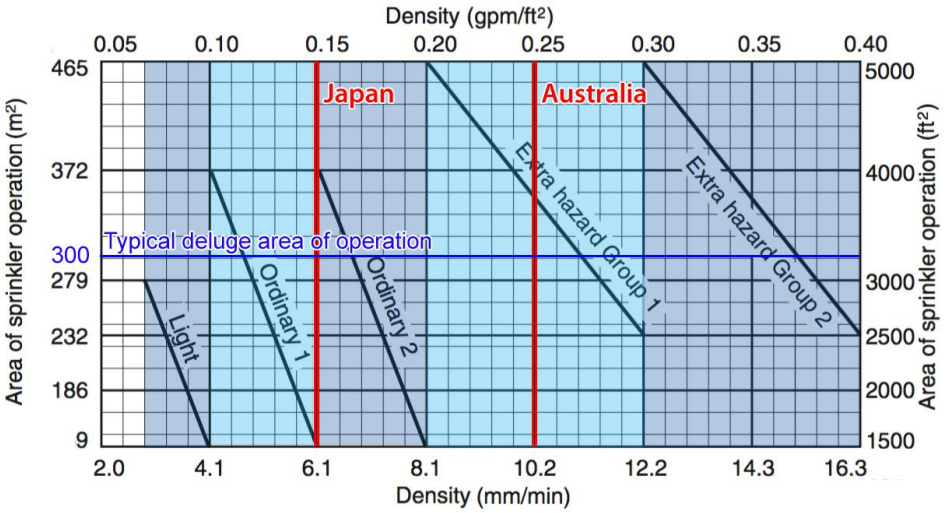

Figure 2.8: Water density versus area of sprinkler operation in NFPA 13 (based on[31])

Essentially NFPA 13 defines 5 hazard categories, which correspond to as many water flow intervals. The upper limit of each water flow interval is given for the smallest sprinkler operation area for a certain hazard classification. As the sprinkler operation area gets bigger, the prescribed water density reduces. The big spread on the prescribed water flows is supposedly linked with the FFFS objective. Five possible objectives or strategies can be defined according to [17]:

- Prevention of fire;
- Extinguishment;
- Suppression;
- Control of burning; and
- Exposure protection.

It can be deduced from figure 2.8 that the Australian requirement will go further than the Japanese in terms of FFFS objective. The Benelux II tunnel, one of the few deluge-protected tunnels in Europe, was tested with a 12 mm/min water flow rate and exceeds even the more conservative Australian prescribed water flow.

Throughout the past decades there has been a few full scale tunnel fire test with FFFS. An overview of some of the most noteworthy experiments is given in table 2.3 and is mostly based on [22]. The experiments labelled as 'Water spray' fire suppression are the ones that utilise a deluge suppression system. Recurring values for the water flow of these water spray experiments are the 6 mm/min and 10 mm/min as prescribed by Japan and Australia and the 12 mm/min as the upper value used in the Singapore tests and the Benelux II test. This translates in the water density interval enclosed by Hazard Category 'Ordinary 2' and 'Extra hazard Group 1' as described by NFPA 13 [31] (see figure 2.8). Numerous deluge experiments [37] conducted in between 1960 and 1990 pointed towards 6 mm/min to be sufficient for fire control and to prevent fire spread [22].

Table 2.3: Overview of full-scale tunnel fire experiments with FFFS (based on [22])

Year	**Test**	**Fire Suppression**	**Water Flow [mm/min]**	**HRR [MW]**
1980	P.W.R.I tunnel Japan	Water spray	6	4.4 - 5
2000 - 2001	Benelux II tunnel The Netherlands	Water spray	12	5 - 30
2002 - 2004	IF tunnel (UPTUN) Norway	Low and high pressure mist	1.1 - 3.3	2 - 25
2004	IF tunnel (Marioff) Norway	High pressure mist	1.4 - 3.7	5 - 25
2006	San Pedro de Annes (Marioff) Spain	High pressure mist	3.7 - 4.3	75 - 90
2008	Sydney Harbour tunnel (AECOM) Australia [2]	Water spray	10	5
2011 - 2012	Singapore tests (Efectis) Spain	Water spray	8 - 12	150
2013	Runehamar tunnel (SP) Norway	Water spray	10	100

The concept of Critical Delivered Density (CFD) or Required Delivered Density (RDD) can be explained with figure 2.9. Upon sprinkler activation at $t_{activation}$ there are essentially two fire scenarios, depending on the water flow, that can follow: growth or suppression. The critical condition is where the heat release rate is controlled. Above this critical water flow suppression occurs and below this water flow the fire will keep growing. Research by

Bilson, Purchase and Stacey [4] has shown that very little water actually reaches the seat of the fire for the case of shielded fires. It would therefore not be realistic to have extinction of the fire as you FFFS objective in tunnels.

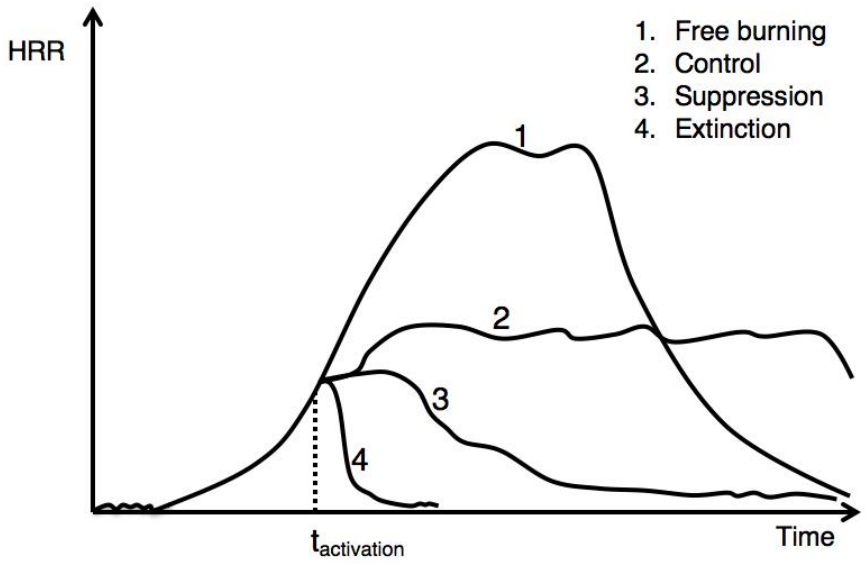

Figure 2.9: Possible fire behaviour after sprinkler activation (based on [47])

There is no research available on required delivered density for tunnel fires. However, there are several studies on the RDD for different experimental settings. Quite extensive research has been carried out on sprinklers for rack storage. The resulting required water flows are usually given for different storage heights and are dependent on the storage category. The Factory Mutual Research Corporation (FMRC) defined several commodity classes in the 90's; Class I to IV with increasing hazard as well as three plastic commodity classes [33]. Table 2.4 gives an overview of these classes and describes how these classes are represented for experiments.

NFPA 13 similarly divides the commodities in four main classes and also defines two classes of plastics; unexpanded and expanded [33]. The plastics are divided in three subclasses; A, B and C; depending on the type of plastic. There are some differences compared to the FMRC classification when it comes to categorization of certain plastics.

The Swedish standards also classify in 4 Categories: L1, L2, L3 and L4 [33]. Category L1 might include commodities I to III from FMRC. This means that the Swedish (European) required level of protection of low hazard

Table 2.4: Standard commodities used as reference for the classification system according to FMRC [33]

FMRC Commodity Class	Standard commodity used as reference
I	Glass jars in compartmented cartons
II	Double tri-wall cartons with steel liner
III	Paper jars in compartmented cartons
IV	Polystyrene and paper jars in compartmented cartons
Cartonated Group B Unexpanded Plastic	
Cartonated Group A Unexpanded Plastic	Polystyrene jars in compartmented cartons
Cartonated Group A Expanded Plastic	

commodities, corresponding to Class I and II, is higher than in the US. Category L2 compares to class III and IV (some commodities would be classified as Unexpanded Plastic). Category L3 compares to Unexpanded Plastic and L4 to Expended Plastic [33]. In general it can be concluded that the aforementioned standards are not identical but do take a similar approach; the total content of plastics defines the commodity classification.

Figure 2.10 shows the relationship between RDD and convective heat release rate for FMRC's standard plastic commodity in more detail. It demonstrates the importance of early sprinkler activation since the required water flow increases with the HRR of the fire.

Table 2.5: Required level of protection according to RUS 120-3 for a storage height of 6.1 m, operation area of 250 to 300 m^2 and a clearance of 3 m[40]

Storage category	Water density [mm/min]
L1	9.2
L2	13.1
L3	21.7
L4	30.0

Clearly, a tunnel car fire is different from a rack fire. There are however several similarities; both types of fire are shielded, both fires contain plastics and both fires are assumed to occur in an enclosure. A car fire is a single shielded fire with far less combustible material than multiply shielded rack fire of several meters. A car fire will be more responsive to sprinklers compared to a rack fire as its geometry is less complex. Therefore, only the least severe rack fires could be used as order of magnitude estimation for

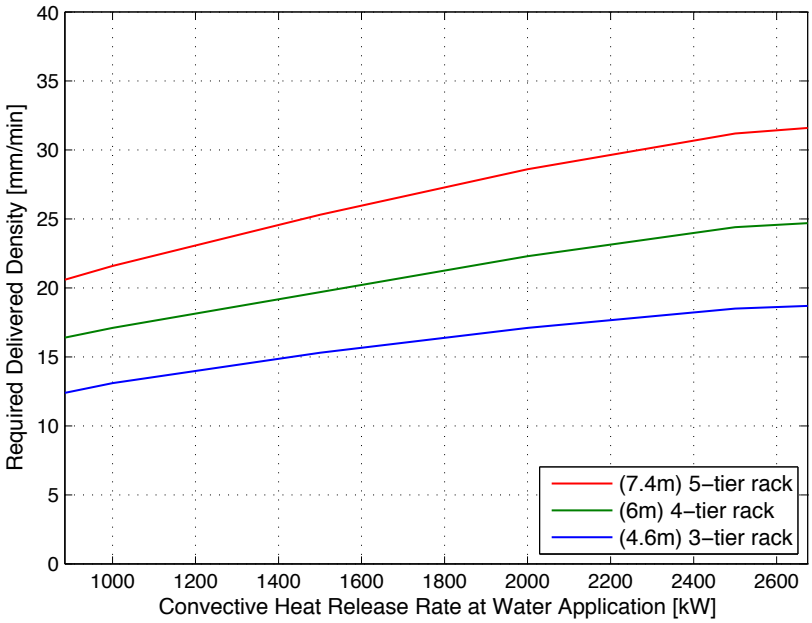

Figure 2.10: RDD values for 3, 4 and 5 tier rack storage of FMRC's plastic commodity based on 10% consumption criteria. [48]

the required water flow to suppress car fires. Summarising tables 2.5, 2.6 and 2.7 suggest that the RDD for car fires could be under 10 mm/min if the latter estimation approach was applied. Additional research [47] was carried out on the FMRC commodities. The results, shown in figure 2.11, confirm the RDD of 6 mm/min for the Class II commodity. Class III, Class IV and the plastic pallet commodities are described to be within the uncertainty range of the experiment and therefore all require a water flow of about 11-12 mm/min in order to be suppressed. Note that the HRR at sprinkler activation is also shown in figure 2.11. These heat release rates are approximately 8 MW; significantly more than what is expected from a single car fire. It is interesting to see how the required water flow changes for changing fuel types. Fuels are in practice relatively constant for car fires, but can differentiate significantly for truck fires. The latter situation is out of the scope of this work since the focus lies on deriving the RDD value for passenger cars.

A Computational Fluid Dynamics (CFD) approach was taken by Harris [17] to determine the RDD for tunnel fires. These Fire Dynamics Simulator (FDS) simulations consisted out of a 30m long tunnel with two identical fuel cribs to replicate a tunnel fire. The only difference between both piles was

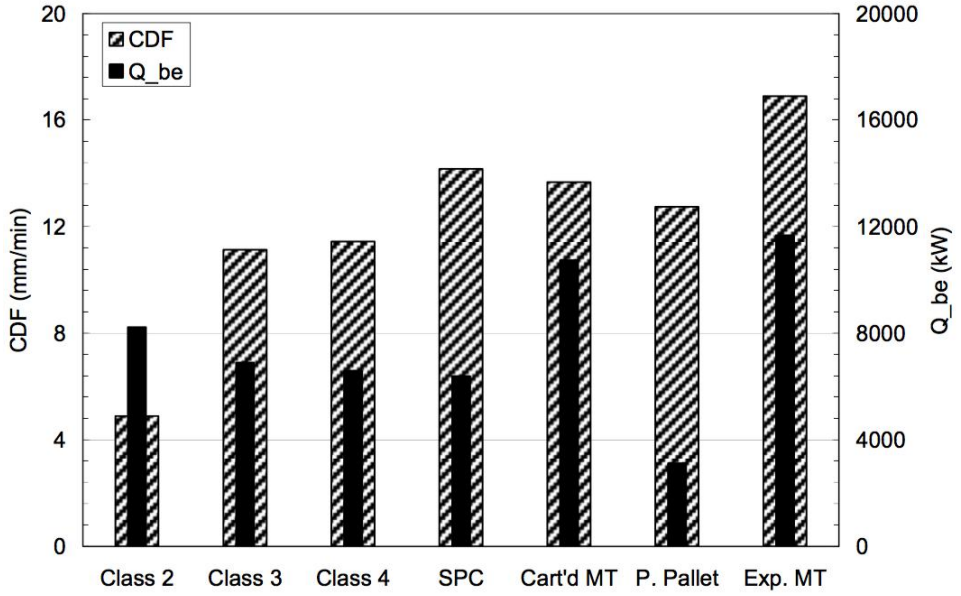

Figure 2.11: Critical Delivered Fluxes for the FMRC commodities [47]

that one pile was unshielded and the other shielded. The latter case would be more representative for a truck or car fire case. The fuel properties were devised in such a way that they would mimic the fire behavior of a medium sized truck. The tunnel cross section was rectangular with a height of 6m and a width of 9m. The deluge system was activated at 12 MW and the results of both fuel cribs are shown in figure 2.12a and 2.12b.

Table 2.6: Required level of protection according to FM Datasheet 8-25 and 8-9 for a storage height of 6.1 m, operation area of 250 to 300 m^2 and a clearance of 3 m [13]

Commodity class	**Water density [mm/min]**
I	6.0
II	6.0
III	7.1
IV	9.7
Plastic A and B non-expanded	24
Plastic A and B expanded	24

Table 2.7: Required level of protection according to NFPA 231 for a storage height of 6.1 m, operation area of 250 to 300 m^2 and a clearance of 3 m[13]

Commodity class	**Water density [mm/min]**
I	7.0
II	7.7
III	9.8
IV	13.2
Plastic A, non-expanded, exposed, stable	18.3
Plastic A, expanded, exposed, stable	20.4

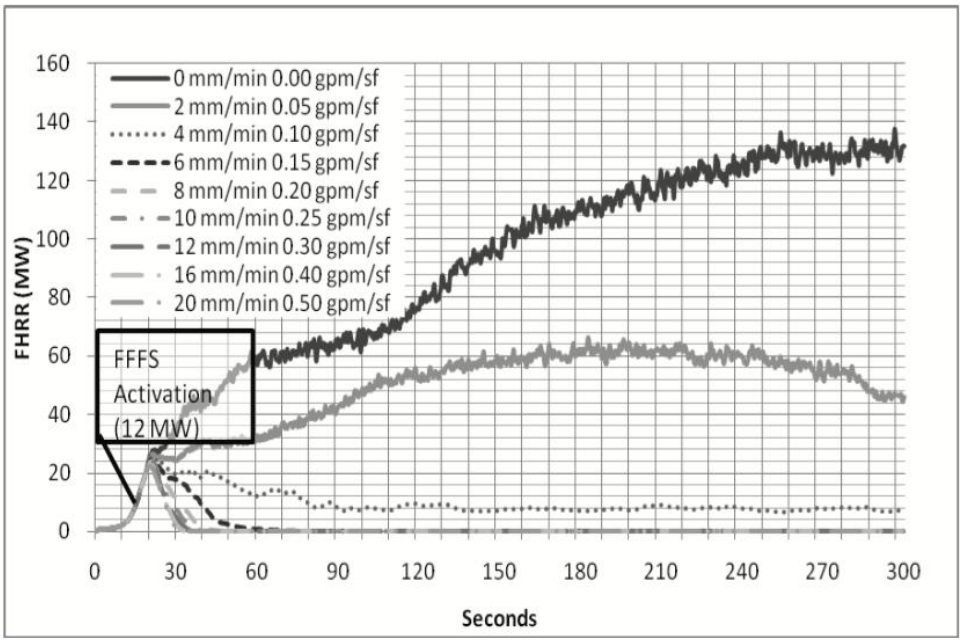

(a) Unshielded fire

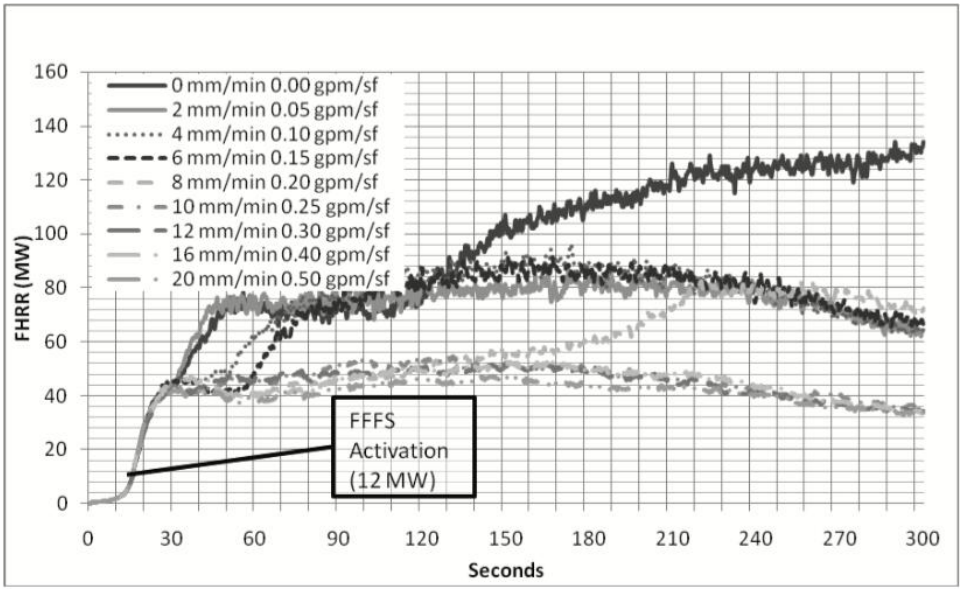

(b) Shielded fire

Figure 2.12: HRR for varying water application rates in case of (a) unshielded and (b) shielded fires [17]

Chapter 3

Methodology

The test program was divided in two experimental stages:

- water distribution tests; and
- car fire tests

The intent of the test method described further is to quantify the influence of the water flow to the burning behaviour of a car fire.

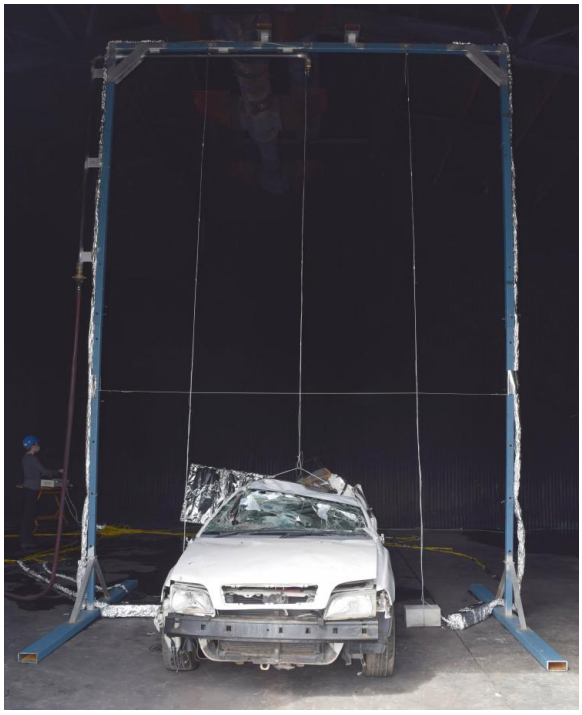

Figure 3.1: Experimental setup

3.1 Experimental Setup

The experimental setup consists out of a single deluge sprinkler nozzle symmetrically aligned above a car. A steel frame was constructed in order to position the nozzle at a height of 5.5m from the ground, as shown in figure 3.1.

3.2 Instrumentation

3.2.1 Thermocouples

Three thermocouple trees were placed at the centre and on both sides of the car (see figure 3.1). The distribution of thermocouples is shown in figure 3.2. The thermocouple tree in the centre will allow for flame height estimation and will help in assessing whether or not the tunnel structure would incur damage. The main purpose of the thermocouple trees on the sides is to determine the risk for fire spread before and after sprinkler activation.

Additionally to the thermocouple trees, four thermocouples are placed inside the car. There is one thermocouple under the roof and the other three are in between the front seats, in the middle of the foot compartment of the backseat and in the middle of the backseat, respectively.

T1 to T5, shown in figure 3.2 are the thermocouples in the vicinity of the car (T1 to T4) and under the roof (T5). These positions will be used in further sections in order to quantify the burning behaviour before, during and after sprinkler activation. It is assumed that the side of T1 and T2 is representative of both sides of the burning car. This is the side of the car that was not cut up for fire fighting purposes.

3.2.2 Video and IR Cameras

Video and infrared (IR) cameras were used throughout the tests. The video cameras enable understanding the different stages of the burning behaviour and will, as long as there is sufficient visibility, help with estimating the flame heights.

As soon as visibility is lost, the IR camera is the sole source of valuable footage. From this footage the flame heights can be determined and, consequently, the heat release rate can be estimated.

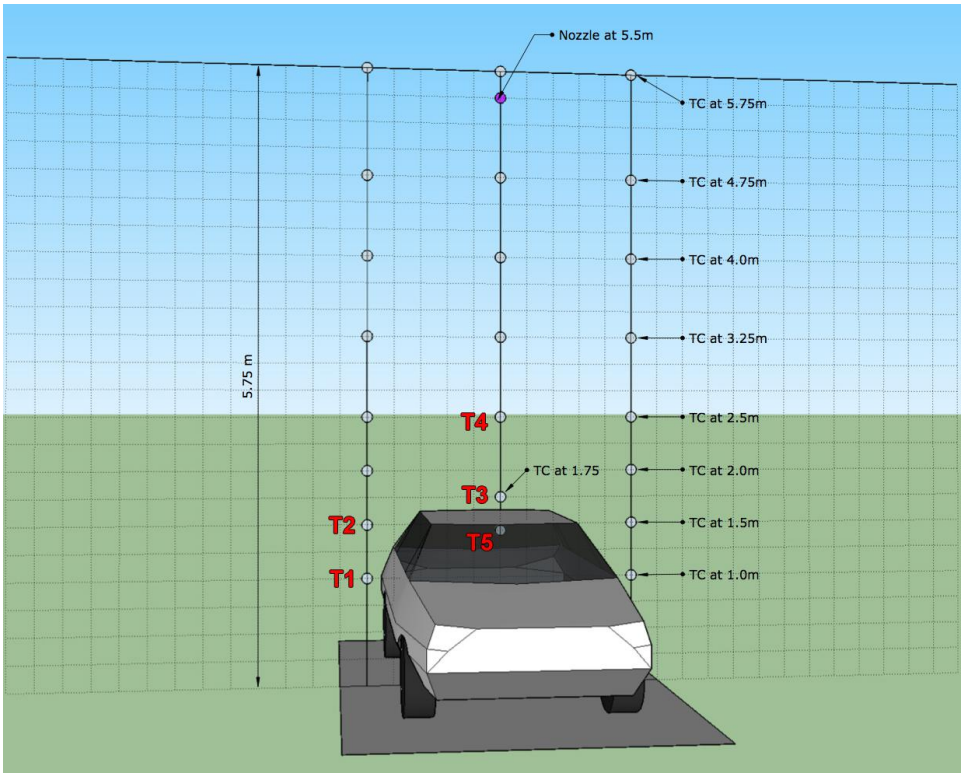

Figure 3.2: Schematic of the test setup

3.3 Water Distribution

A BETE nozzle type N9W20.4 (See figure 3.3), is used in a single-nozzle configuration. The water flow from the nozzle is directly related to the pressure of the system. This relationship is expressed in equation 3.1.

$$FlowRate = K\sqrt{p} \qquad [\mathrm{l/\,min}] \quad (3.1)$$

In this equation, p is the pressure in bar and K is the factor correlating the system pressure with the water flow. This K-factor is reported by the manufacturer. This relationship is shown in figure 3.4 for the nozzle used in the experiments. This flow is distributed over an area with a coverage diameter D and is dependent on the system pressure, installation height and spray angle.

In reality there is no deluge nozzle that can evenly distribute the nozzle water flow over the covered area. In order to determine the distribution of the water flow at ground level, a series of standard 'pan tests' [41] was carried out. In these kind of tests, square pans are placed along the radius

Figure 3.3: BETE N9W20.4 deluge nozzle

away from the sprinkler nozzle (see figure 3.5). After a certain discharge time, the water flow at these discrete points away from the sprinkler head can be derived by measuring the height of water in each pan and dividing it by the discharge time.

The pan test shown in figure 3.5 consists out of a strict procedure to ensure consistency. First, a plastic sheet is placed on the boxes while the system activates. In this manner, any distortion during ramp-up of the system pressure is avoided. After stabilisation at the requested system pressure, the sheet is removed. The square pans, with dimensions of 356x356x292H [mm], will then collect water during a 10 min time span. For system pressures of 7 bar and up, a shorter time span is used as the boxes would overflow before 10 min. After the boxes are covered again, the system pressure is dropped. The height of water in every box is measured with a ruler and later divided by the time span to determine the water flow in mm/min.

The water flow distribution at various pressures was measured with pans placed in one direction from the centre. In order to assess the radial symmetry of the water distribution, additional pan tests were performed for two pressures in 45°increments. The setup of these tests is shown in figure 3.6.

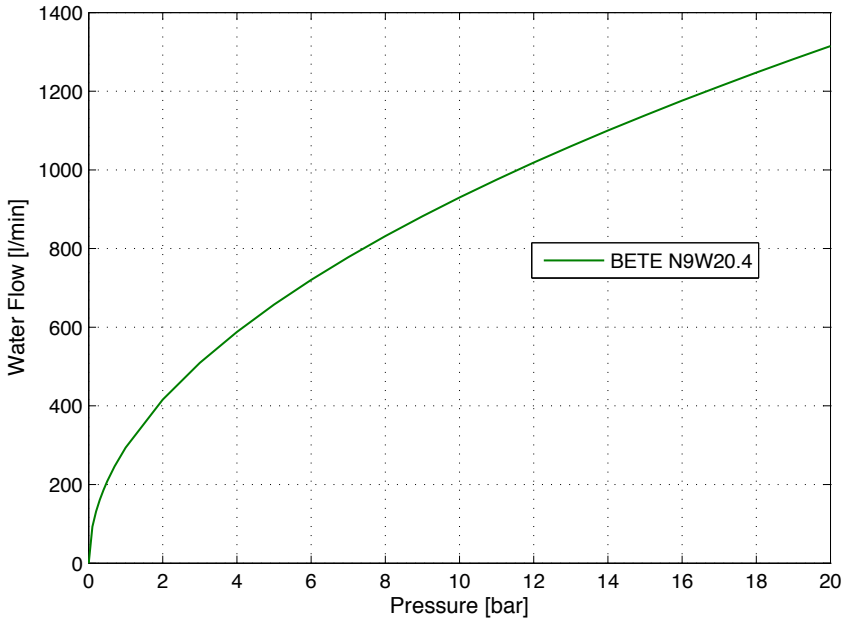

Figure 3.4: Relationship between the nozzle water flow and the system pressure

Figure 3.5: 'Pan test' to derive water distribution

Figure 3.6: Diagonal 'Pan test' to assess radial symmetry

3.4 Car Fire

3.4.1 Ignition Source

A bag of woodchips drenched in diesel, shown in figure 3.7, was used as the source of ignition. This ignition source was placed in the middle of the foot compartment of the backseat. This is not necessarily the most likely, but serves as a worst case scenario.

Figure 3.7: Ignition source used in the experiments

Another potential fire scenario is that of an engine fire. The fire barrier between the engine and the inside of the car would compartment the fire and hence limit the HRR. In older cars this fire barrier is less reliable, but even in modern cars this barrier can fail following a crash. Therefore, the engine fire is omitted and the case of a fire inside the passenger compartment is chosen to be the worst credible case.

3.4.2 Fuel Load

The main fuel load in cars are the seats, interior lining, plastics in the finishing or the body work, the tyres and the fuel from the vehicle tank. The latter is not present for the purpose of this experiment. It is a possibility that the fire barrier between the engine and the passenger compartment fails. In that case, additional fuel from cabling and other combustibles from the engine compartment are added to the fuel load. The doors of the tested cars are removed prior to the test but placed inside the car to maintain the same fuel load.

3.4.3 Heat Release Rate

In order to estimate the HRR from the flame height, the mean flame height needs to be measured. This is required since the intermittent part of the flame fluctuates several times per second and an instantaneous analysis would therefore not resemble the heat release rate of the fire. The mean flame height is found by collecting the flame height of 100 infrared frames (4 seconds at 25 FPS) and developing a cumulative normal distribution. The mean flame height is the height that corresponds with a probability of 0.5.

The SFPE Handbook of Fire Protection Engineering [18] provides Heskestad's flame height correlation. This is the method used to derive heat

release rates from the mean flame heights in this thesis. This relationship is given in equation 3.2 where D [m] is the diameter of the fire and $\dot{Q}$ is the heat release rate [kW].

$$L = -1.02D + 0.235\dot{Q}^{2/5} \quad \text{[m]} \quad (3.2)$$

Rearranging this equation for the HRR gives:

$$\dot{Q} = \left(\frac{L + 1.02D}{0.235}\right)^{5/2} \quad \text{[kW]} \quad (3.3)$$

The flame length L [m] is derived from the IR camera recordings and the fire diameter D [m] is assumed to be the width of the car.

Chapter 4

Results

This section gives an overview of the most significant experimental results. First, the results from the water distribution tests are shown and second the resulting heat release rates from the flame length analysis are shown. Lastly, the thermocouple data shows how the fire is affected by sprinkler activation. For the assessment of the burning behaviour of the car, the main focus lies on thermocouples T1-T5. Their respective locations are shown in figure 4.1. In the assessment of these thermocouples, a conservative approach is used; e.g. if one temperature drops slightly, but another one rises, the 'temperature in the immediate vicinity of the car' is assumed to rise. An instant drop in temperature is defined as a drop to below 100°C during the first 20 seconds of sprinkler activation. A gradual drop is a drop that occurs over a longer period of time.

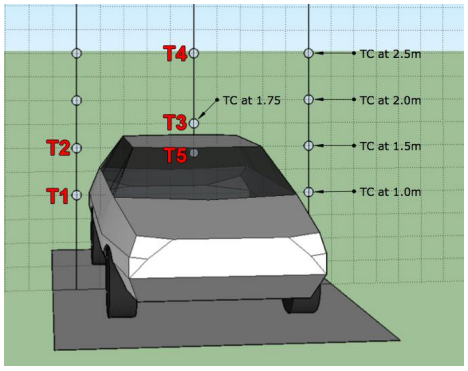

Figure 4.1: Positions of thermocouples T1-T5 in the vicinity of the car

It is important to mention that the tabular temperature data of T1 to T5, mentioned throughout this chapter is taken instantaneous. In order to interpret these numbers and to understand the underlying trend it is essential that they are used in conjunction with their corresponding time-temperature plots.

4.1 Water Distribution

The variation of the water flow along the radius away from the sprinkler nozzle is shown in figure 4.3a. A trend can be deduces; from a single peak for the highest system pressure towards a double water flow peak for lower pressures. The variation along the radius away from the nozzle confirms that the water distribution on the ground cannot be found by simply dividing the nozzle flow rate with the coverage area. A visual representation of the water distribution corresponding with 6 bar system pressure is shown in figure 4.4.

In order to assess the water distribution independently from the nozzle water flow, this graph is normalized. Essentially the curves are divided by the nozzle flow rate shown in figure 3.4. The resulting normalized graph is shown in figure 4.3b.

Note that figure 4.3a gives the water distribution in one direction only. The two-dimensional water distribution grid for 6 and 7 bar is shown in figure 4.2. These plots are based on tests from 8 different directions with a 45 degrees interval. The results for 6 and 7 bar are shown in figure 4.2.

In a realistic tunnel deluge system there will never be a single-nozzle configuration. There will always be an overlap between the coverage areas of adjacent deluge nozzles. The water distribution for the case of 3, 4 and 5m nozzle spacing is shown in Appendix A. These graphs are found by mirroring the distributions from figure 4.3a and summing the water flows that overlap.

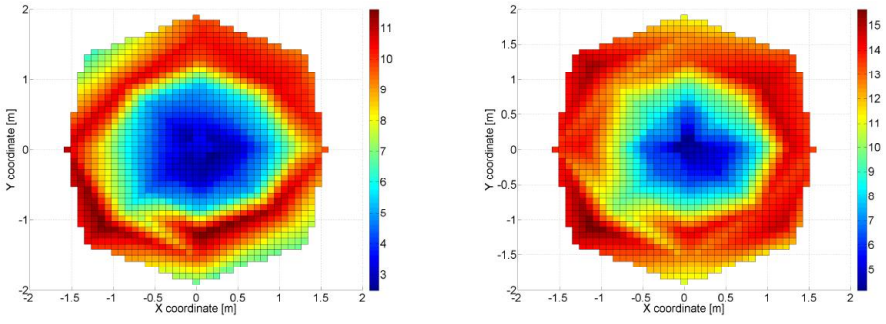

(a) 6 bar **(b)** 7 bar

Figure 4.2: Radial water flow distribution for 6 and 7 bar of system pressure

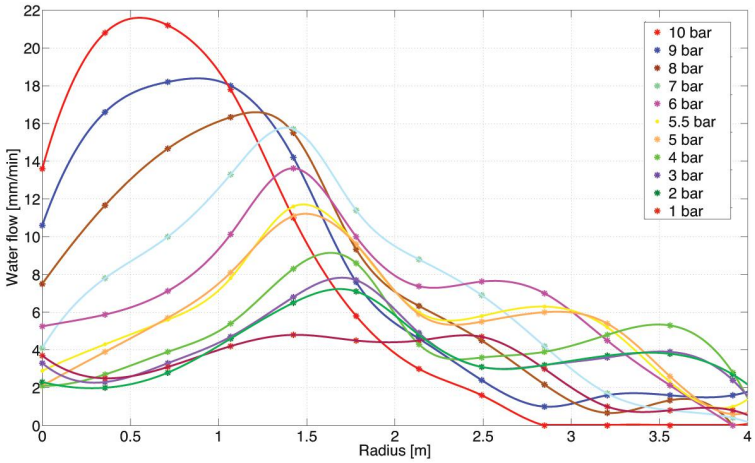

(a) Water flow distribution

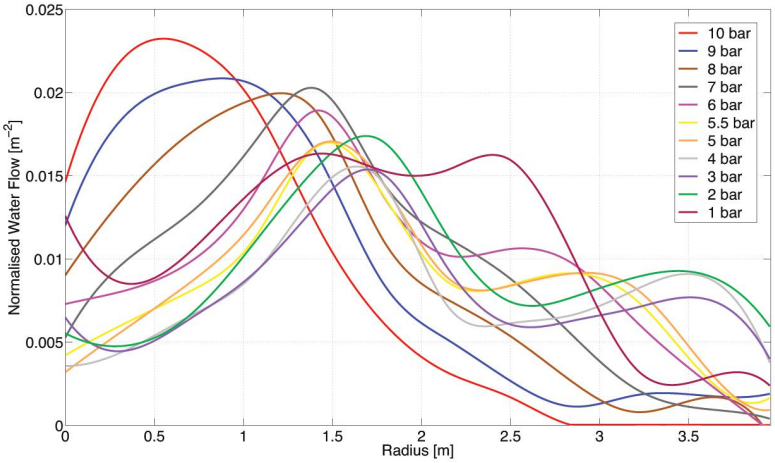

(b) Normalised water flow distribution

Figure 4.3: Resulting water flow distribution from the pan tests

It can be concluded from figure 4.2 that the radial symmetry assumption is applicable. In essence this means that every graph in figure 4.3a can be rotated along its origin to form the 3D water distribution. In order to find the representative water flow for a certain system pressure it is assumed that a car fire is roughly equivalent to a pool fire with a diameter of 2m. This means that the water flow values from figure 4.3a must be integrated from the origin to the 1m radius mark. Since the integration of the water flows is carried out for a radius equal to unity, the resulting numerical values is the previously mentioned 'representative water flow'. The result of this integration is shown in table 4.1.

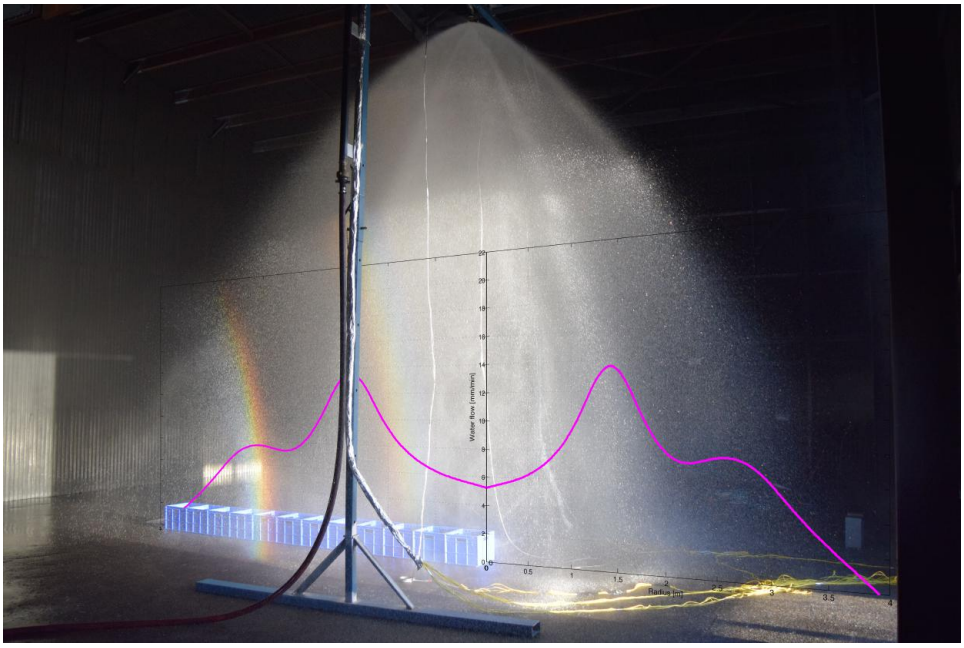

Figure 4.4: Visual representation of water distribution for 6 bar

Table 4.1 is graphically shown in figure 4.5. As can be seen from figure 4.3a, for the 0 to 1m radius interval, the water flow for 1 bar is in fact higher than those of 2 and 3 bar. 1 bar of system pressure is not enough to create a pressurised water umbrella with the same radius. As a consequence, there is a significantly larger amount of water falling closer to the centreline than is the case for 2 bar.

Table 4.1: System pressure with corresponding water flow on the car area

Pressure [bar]	Water Flow [mm/min]
1	3.0
2	2.5
3	3.0
4	3.3
5	4.7
5.5	4.9
6	6.6
7	8.6
8	12.6
9	16.6
10	19.8

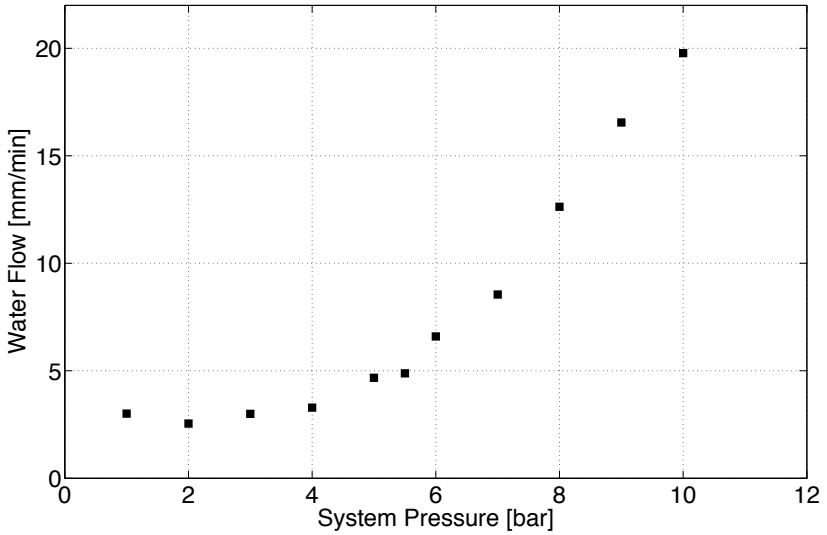

Figure 4.5: Averaged water flows for 2m diameter (car area)

4.2 Fire Size

Heskestad's correlation in the form of formula 3.3 is used to derive HRR values from the flame height recordings. Figure 4.6 shows the cumulative normal distribution of the flame height for 100 frames before the first sprinkler activation in test 1. This figure shows how the intermittent flame affects the instantaneous flame height. It is the flame height with 50% probability that is referred to as mean flame height. The mean flame heights at every sprinkler activation are summarised chronologically in table 4.2. The HRR column of that same table shows what heat release rate this is equivalent to, according to Heskestad's correlation. The average width of the cars, 1.8m, is used as representative fire diameter in that correlation. Note that the values for the HRR are not peak release rates, but the heat release rates at which the deluge system was manually activated.

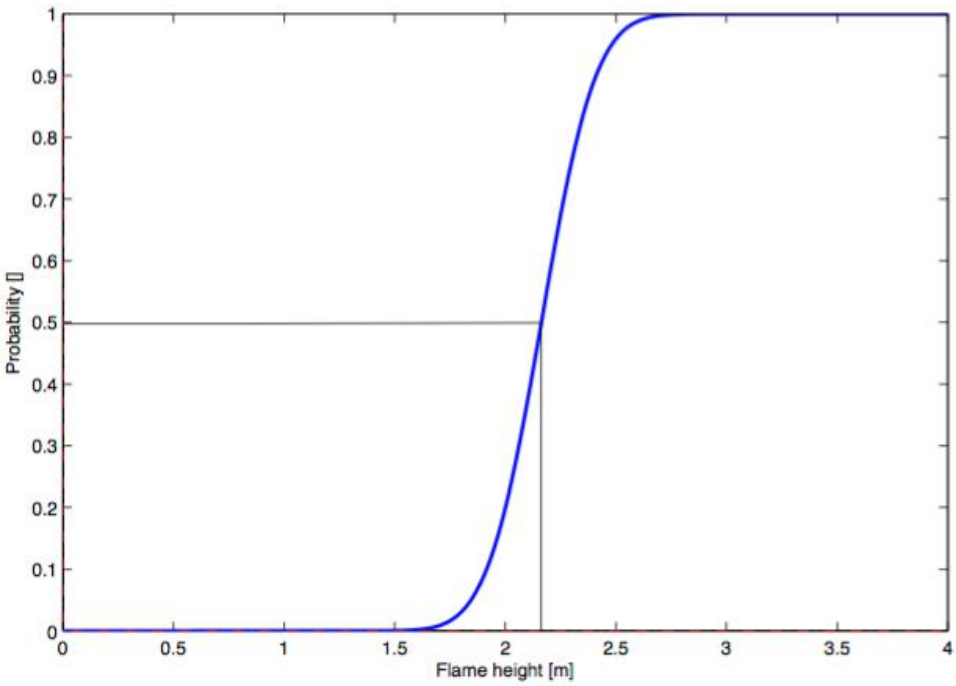

Figure 4.6: Cumulative normal distribution for the flame height of Test 1 at first sprinkler activation

Table 4.2: Heat Release Rates at deluge activation from equation 3.3 [Heskestad]

Test	Time [s]	Mean Flame Height [m]	HRR [MW]
1	290	2.16	1.19
1	420	3.00	1.92
2	120	3.42	2.37
2	180	3.73	2.73
2	300	1.81	0.95
2	510	2.11	1.15
2	720	1.61	0.82
2	1605	1.16	0.58
2	1877	1.16	0.58
3	100	2.37	1.36
3	260	2.95	1.87
3	475	1.73	0.89
4	75	1.94	1.04
4	300	1.39	0.70
4	720	1.19	0.59
5	145	1.71	0.88
5	320	2.49	1.45
5	480	1.49	0.75
5	1260	2.04	1.11
5	1485	1.61	0.82
5	2005	1.48	0.75
5	2340	1.02	0.52

4.3 Test 1: Volvo S40 Jul '96

4.3.1 Description

In test 1, two water flows were tested on a burning Volvo S40 (Jul '96). Figure 4.7a shows the car right after ignition and the fire size at approximately 250 seconds after ignition is shown in figure 4.7b.

(a) Right after ignition **(b)** At approximately 250s

Figure 4.7: Volvo S40 at ignition and after 250s of fire growth

4.3.2 Timeline of Events

First activation

The first activation of the deluge system occurred when the fire had a mean flame height of 2.16m. The corresponding HRR of 1.19 MW underwent a deluge activation of 2.5 mm/min during 100 seconds. The temperatures next to the car kept rising and the temperatures above the car dropped slightly (see table 4.3).

Second activation

The deluge system was activated a second time with 8.6 mm/min on a fire with mean flame height of 3.00m or equivalent 1.92 MW heat release rate. The deluge system remained active for 300 seconds. As a result of the deluge activation, the temperatures around the car gradually dropped.

4.3.3 Measurements

Table 4.3 shows how the temperatures at the four thermocouples around the car (T1 to T4) and the one underneath the roof (T5) are affected by deployment of the deluge system. After deployment of 2.5 mm/min on a 1.19 MW fire during 100 seconds, the temperatures have not dropped significantly. In fact, the temperature right next to the car has risen from

257°C to 417°C during this time. Only at the thermocouples right above the car, T3 and T4, a temperature drop can be observed.

The second sprinkler activation occurs when the fire is about 1.9 MW. The 8.6 mm/min manages to drop all temperatures around the car from 272-511°C to about 45°C. Furthermore, a drop of over 460°C is recorded right underneath the roof. Table 4.3 shows the impact of the sprinkler system for the second activation.

The different behaviour of the fire after the two sprinkler activations is further demonstrated in figure 4.9. The second activation brings both the temperatures at the centre and at the sides gradually down to a uniform 50°C. The situation for the first activation is very different: the temperatures right above the car are lowered whereas the temperatures on the side, like T1 at 1m height, rise significantly.

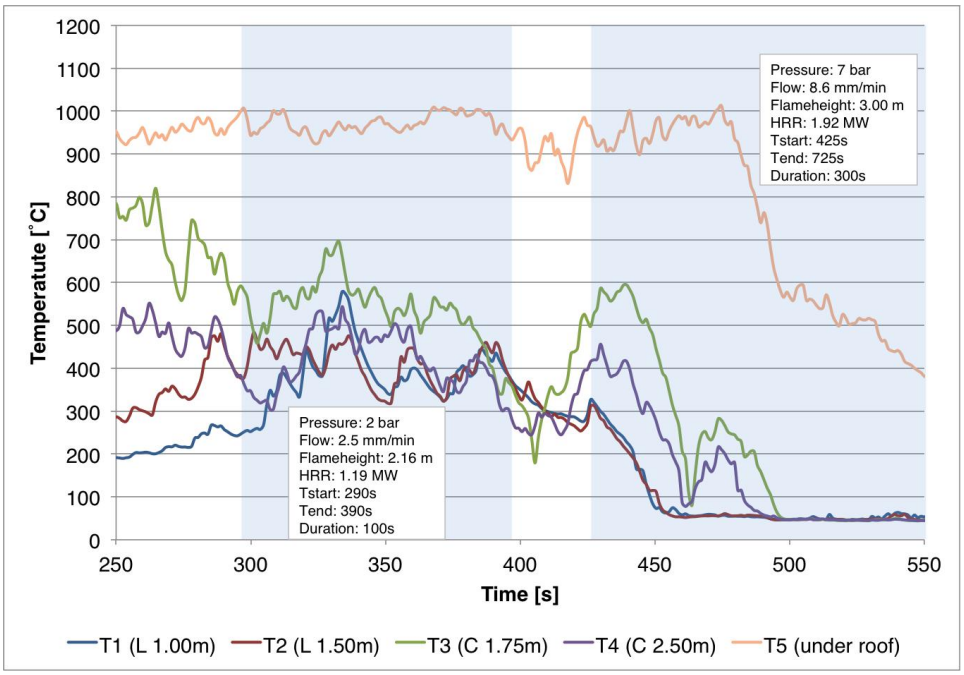

Figure 4.8: Temperature-time curves for Test 1 (Full graph in Appendix B.1)

Table 4.3: Impact of the deluge system for Test 1

	Time	T1 [°C]	T2 [°C]	T3 [°C]	T4 [°C]	T5 [°C]
1.19 MW	t_{290}	257	452	652	463	949
2.5 mm/min	t_{390}	417	437	401	380	979
1.92 MW	t_{425}	292	272	511	397	967
8.6 mm/min	t_{525}	47	46	45	46	506

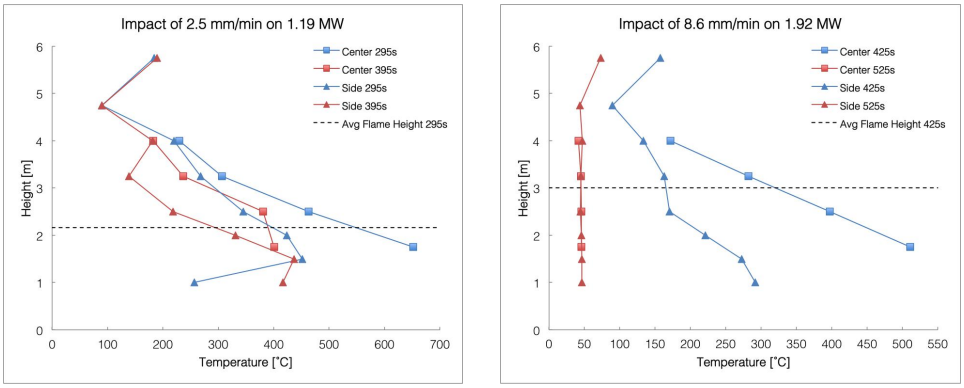

(a) Test 1.1 **(b)** Test 1.2

Figure 4.9: Temperature profiles for Test 1

4.4 Test 2: Saab 9000 CD Jun '94

4.4.1 Description

Test 2 assessed the influence of the deluge system on a burning Saab 9000 CD Jun '94. Figure 4.10a shows the car before ignition and figure 4.10b shows the car during the first sprinkler activation. In this test a total of six sprinkler activations occurred of which the first three are discussed in depth in the following sections. The remaining three activations instantly bring the temperatures around the car down to below 100 °C.

(a) Before ignition **(b)** During first activation

Figure 4.10: Saab 9000 CD before ignition and during the first activation

4.4.2 Timeline of Events

First activation

The first activation of the deluge system occurred when the fire had a mean flame height of 3.42m. The corresponding HRR of 2.37 MW underwent a deluge activation of 3.3 mm/min during 50 seconds. The temperatures above the car kept rising (See figure 4.11).

Second activation

The deluge system was activated a second time with 6.6 mm/min on a fire with mean flame height of 3.73m or equivalent 2.73 MW heat release rate. Figure 4.11 shows that, as a result of the deluge activation, the temperatures around the car gradually dropped during the 100 seconds of deluge activation.

Third activation

The third deluge activation of 14.1 mm/min was activated when the mean flame height was 1.81m (0.95 MW). A water flow of 8.6 mm/min made the temperatures above the car drop instantly. As can be seen from figure

4.11, the temperature right next to the car rises before dropping instantly after about one minute. This is likely to be linked to the steam initially pushing the flame down; effectively enhancing the burning and increasing the temperatures next to the car.

4.4.3 Measurements

Figure 4.11 shows the most significant sprinkler activations for the second test. The full set of sprinkler activations can be found in Appendix B.2. The temperature data at the start and end of every sprinkler activation for test 2 is shown in table 4.4.

The first sprinkler activation of 3.3 mm/min when the fire was 2.37 MW was not able to stop fire growth. It manages to keep T1 and T2 (right next to the car) under 70°C but from T3 and T4 it can be seen that the fire continues to grow.

The second sprinkler activation occurs when the fire is 2.73 MW; the highest recorded HRR during the experiments. Figure 4.11 demonstrates how the 6.6 mm/min of water flow manages to decrease the fire size. However, after a period of 100s, the fire is still not contained inside the car as can be seen from temperature T3 right above the car. Given the downward trend, it is expected for the fire to be contained if the sprinkler system would have been active for just a bit longer.

The third sprinkler activation of 8.6 mm/min at 0.95 MW shows a clear drop in temperatures. After about 20 seconds; the temperature right above the car, T3, drops from 500°C to under 60°C. T1, right next to the car, manages to increase initially but drops from 242°C to 59°C eventually. The temperature underneath the roof drops from 1004°C to 637°C.

The fourth fire size is slightly bigger than the third; 1.15 MW instead of 0.95 MW. However, for this fire size the highest water flow of 14.1 mm/min was used. The temperatures instantly drop from 258-371°C around the car to 44-56°C. The drop in temperature under the roof is bigger than for the third sprinkler activation: from 999°C to 412°C.

The fifth and sixth sprinkler activation constitute as instant temperature drops as a result of the deluge system. Relatively high water flows were used for these smaller fire sizes. The exact impact of the temperatures around the car and under the roof is given in table 4.4.

The temperature profiles for test 2 are shown in figure 4.12. There are essentially two after-sprinkler scenarios for the second test: one at which uniform temperatures of around 50°C are achieved over the entire section

and another where the sprinkler system does not manage to bring down the temperatures at the centreline. The first case is shown in figures 4.12c and 4.12d. Activation 1 and 2 are examples of the second case and are shown in figures 4.12a and 4.12b. However, by looking at figure 4.11, it can be seen that there is a downward trend in the temperatures at the centre. This suggests that over time the second activation could achieve a similar after-sprinkler scenario when given more than 100 seconds.

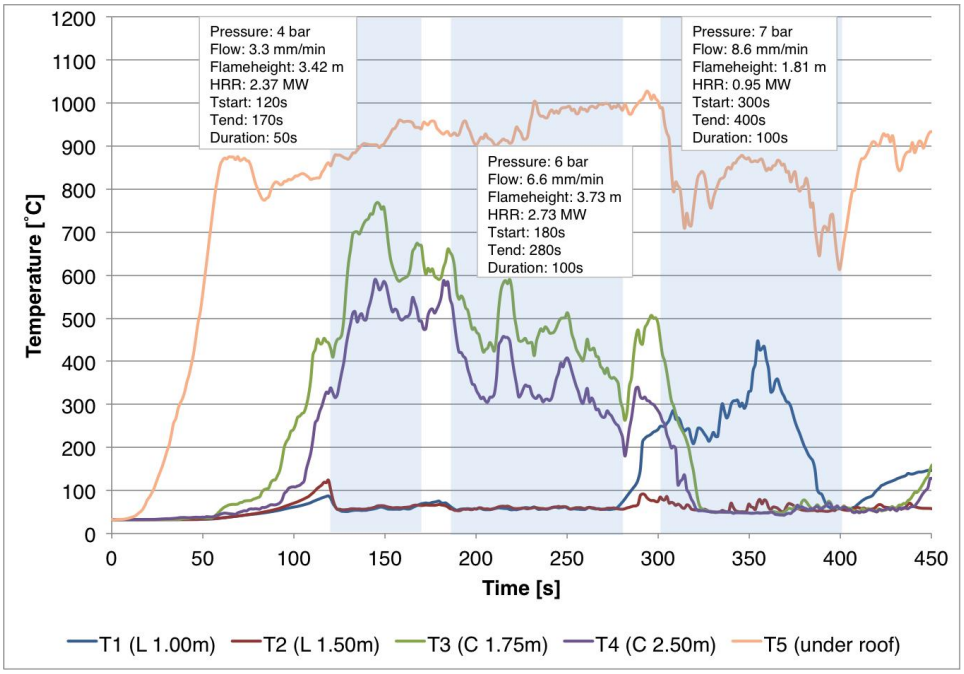

Figure 4.11: Temperature-time curves for the first three sprinkler activations of Test 2 (Full graph in Appendix B.2)

Table 4.4: Impact of the deluge system for Test 2

	Time	T1 [°C]	T2 [°C]	T3 [°C]	T4 [°C]	T5 [°C]
2.37 MW	t_{120}	82	102	429	338	854
3.3 mm/min	t_{170}	69	65	669	493	941
2.73 MW	t_{180}	75	67	590	533	937
6.6 mm/min	t_{280}	74	56	291	222	984
0.95 MW	t_{300}	242	75	488	286	1004
8.6 mm/min	t_{400}	59	56	59	59	637
1.15 MW	t_{510}	266	329	371	258	999
14.1 mm/min	t_{610}	56	53	49	44	412
0.82 MW	t_{720}	118	51	143	165	740
14.1 mm/min	t_{820}	47	43	40	38	375
0.58 MW	t_{1600}	48	33	67	90	89
6.6 mm/min	t_{1700}	38	32	33	31	57

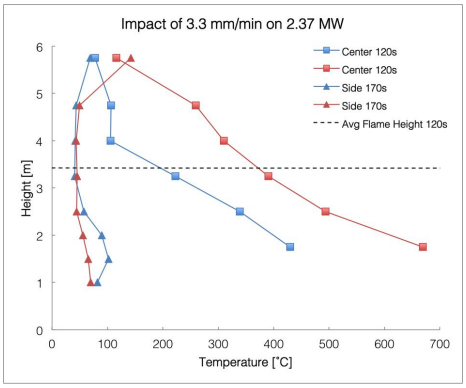

(a) Test 2.1

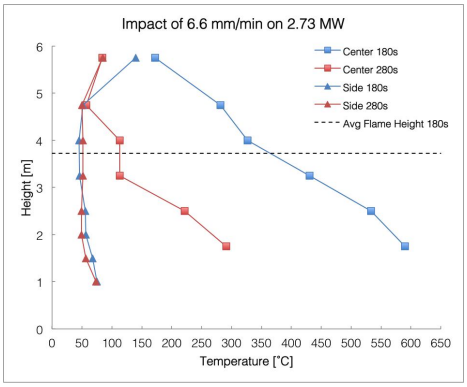

(b) Test 2.2

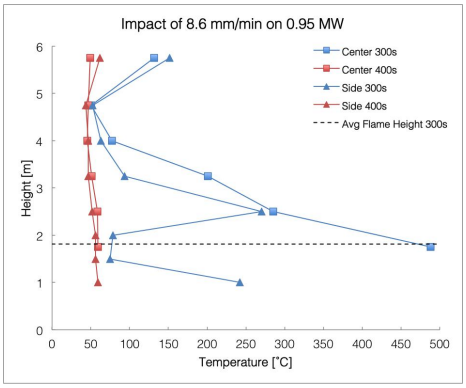

(c) Test 2.3

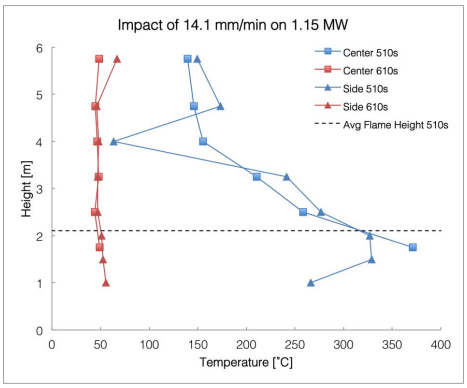

(d) Test 2.4

Figure 4.12: Temperature profiles for Test 2 (Full list in Appendix C.2)

4.5 Test 3: Honda Civic GL Sep '91

4.5.1 Description

In the third test a '91 Honda Civic GL is burned and three different water flows are tested for the deluge system. Figure 4.13 shows the car before ignition and during the first deluge activation. The first two activations are discussed in this section. The third activation is an example of instant temperature drop of a relatively small fire (See Appendix B.3).

(a) Before ignition **(b)** During 4.7 mm/min

Figure 4.13: Honda Civic GL before ignition and at the beginning of the first activation

4.5.2 Timeline of Events

First activation

The first activation of the deluge system occurred when the fire had a mean flame height of 2.37m. The corresponding HRR of 1.36 MW underwent a deluge activation of 4.7 mm/min during 100 seconds. The temperatures right above the car kept rising.

Second activation

The deluge system was activated a second time with 14.1 mm/min on a fire with mean flame height of 2.95m and equivalent 1.87 MW heat release rate. The deluge system remained active for 100 seconds. As a result of the deluge activation, all the temperatures in the immediate vicinity of the car instantly dropped.

4.5.3 Measurements

Figure 4.14 shows the effect of the first two sprinkler activations of test 3. The first attempt at 1.36 MW with 4.7 mm/min shows that the water flow manages to cool the area right next to the car (T1 and T2). However, it

does not succeed in containing the fire within the car enclosure. This can be seen from the T3 and T4 temperature readings (above the car) that rise from 188-107°C to 387-196°C, respectively (see table 4.5). The temperature underneath the roof rises from 808°C to 911°C.

The second sprinkler activation uses 14.1 mm/min on a 1.87 MW fire. An immediate drop in temperature can be witnessed just after about 20 seconds (See figure 4.14). All temperatures around the car stabilize at around 40-60°C. There is a drop of about 500°C underneath the roof. This drop occurs gradually during the 100 seconds of sprinkler activation.

From the temperature profiles shown in figure 4.15 the same two after-sprinkler scenarios from test 2 can be witnessed. The first activation only manages to cool the side temperatures to a uniform 50°C whereas the temperatures at the centreline increase over the entire section. The water flow of 14.1 mm/min lowers all temperatures to a uniform temperature (See figure 4.15b) and figure 4.14 demonstrates it does so after about 20 seconds.

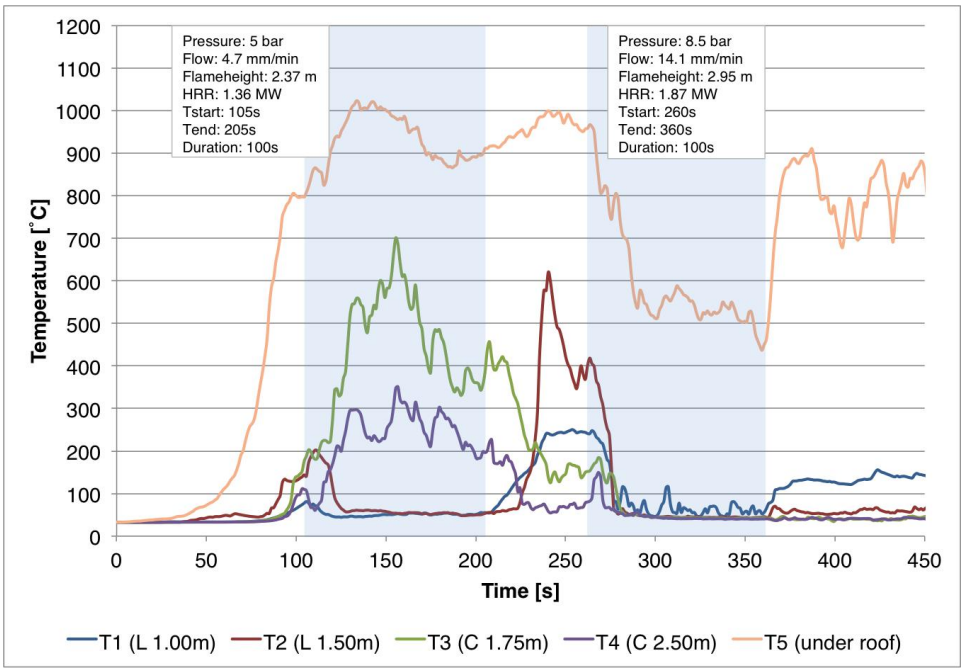

Figure 4.14: Temperature-time curves for the first two sprinkler activations of Test 3 (Full graph in Appendix B.3)

Table 4.5: Impact of the deluge system for Test 3

	Time	T1 [°C]	T2 [°C]	T3 [°C]	T4 [°C]	T5 [°C]
1.36 MW	t_{105}	81	141	188	107	808
4.7 mm/min	t_{205}	55	54	387	196	911
1.87 MW	t_{260}	245	400	138	67	953
14.1 mm/min	t_{360}	56	46	43	40	450
0.89 MW	t_{475}	148	212	63	43	702
8.6 mm/min	t_{575}	46	40	40	39	225

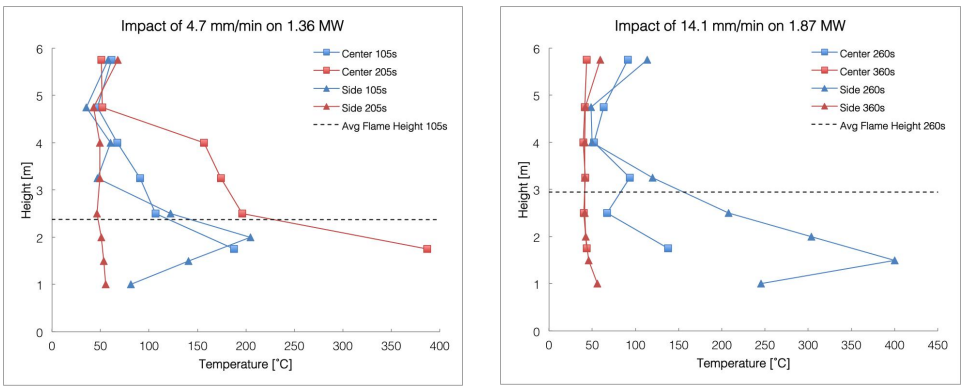

(a) Test 3.1 **(b)** Test 3.2

Figure 4.15: Temperature profiles for Test 3 (Full list in Appendix C.2)

4.6 Test 4: Mazda 323 Aug '92

4.6.1 Description

Three deluge activations were used on a '92 Mazda 323. Figure 4.16 shows the car before ignition and at the beginning of the first activation.

(a) Before ignition **(b)** Beginning of first activation

Figure 4.16: Honda Civic GL before ignition and at the start of the first deluge activation

4.6.2 Timeline of Events

First activation

The first activation of the deluge system occurred when the fire had a mean flame height of 1.94m. The corresponding HRR of 1.04 MW underwent a deluge activation of 4.7 mm/min during 100 seconds. The temperatures right above the car kept rising.

Second activation

The deluge system was activated a second time with 14.1 mm/min on a fire with mean flame height of 1.39m and equivalent 0.70 MW heat release rate. The deluge system remained active for 100 seconds. As a result of the deluge activation, all temperatures in the immediate vicinity of the car instantly dropped.

4.6.3 Measurements

During the first deluge activation of test 4, the temperature readings right above the car (T3 and T4) rise from 185-110°C to 280-309°C, respectively (See Table 4.6). However, the water spray manages to cool the area right next to the car to about 60°C. The cooling of the sides and the heating of the centre temperatures over the height can be observed from figure 4.18a.

The temperature underneath the roof grows from just below to just over 1000°C.

Because of the rather long waiting time between the first and second activation, the temperatures right next to the car are the highest recorded for this position at 453-601°C. The given water flow manages to drop these, as well as the 386-220°C temperatures right above the car, to just over 40°C within 20 seconds (see figure B.4 table 4.6). The overall drop in temperature along the height is shown in figure 4.18b. There is a temperature drop underneath the roof of about 490°C: from 942°C to 449 °C.

The third activation occurred when the fire was 0.59 MW (See Appendix B.4). A water flow of 8.6 mm/min made all the temperatures around the car drop to around ambient (35°C). The temperature underneath the roof dropped gradually from 221°C to 105°C.

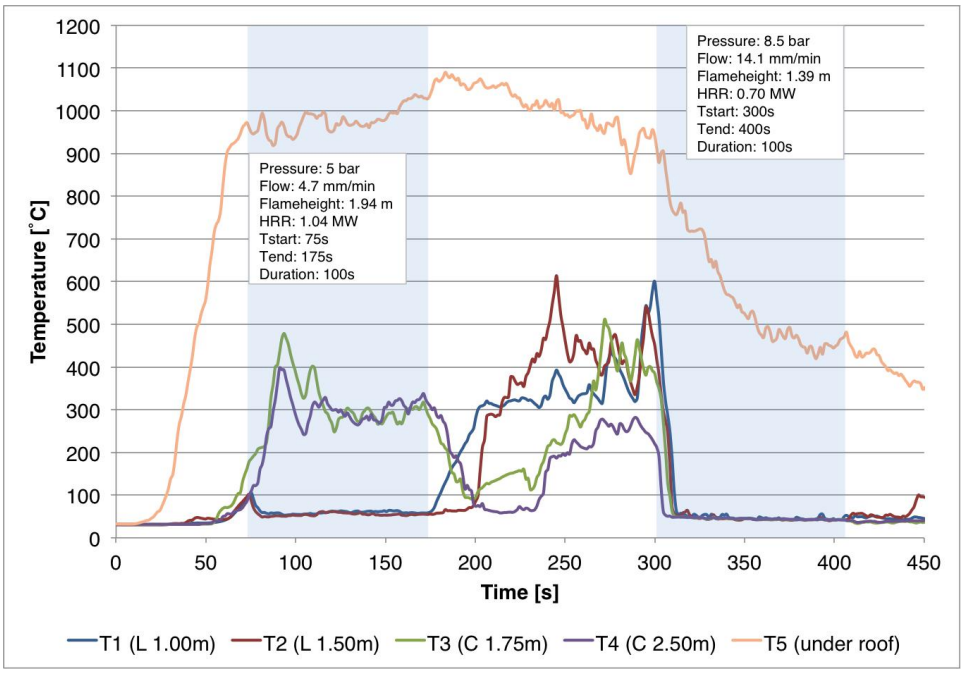

Figure 4.17: Temperature-time curves for the first two sprinkler activations of Test 4 (Full graph in Appendix B.4)

Table 4.6: Impact of the deluge system for Test 4

	Time	T1 [°C]	T2 [°C]	T3 [°C]	T4 [°C]	T5 [°C]
1.04 MW	t_{75}	106	86	185	110	949
4.7 mm/min	t_{175}	60	56	280	309	1037
0.70 MW	t_{300}	601	453	386	220	942
14.1 mm/min	t_{400}	42	42	42	42	449
0.59 MW	t_{720}	81	145	218	143	221
8.6 mm/min	t_{820}	36	35	36	35	105

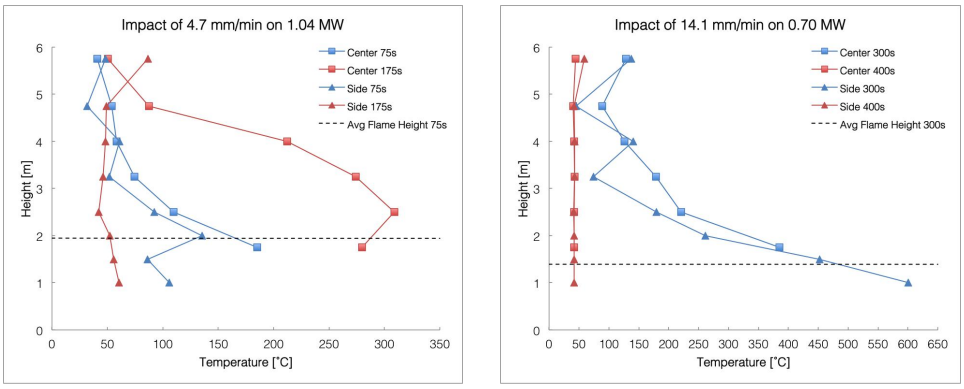

(a) Test 4.1 **(b)** Test 4.2

Figure 4.18: Temperature profiles for Test 4 (Full list in Appendix C.2)

4.7 Test 5: Holden VT Station Wagon Dec '99

4.7.1 Description

A total of seven deluge activations were applied on a Holden VT Station Wagon from '99. The first three are looked into in more detail in the following sections. The remaining four activations are very similar; in each of those cases the temperature instantly dropped after deluge activation. An overview of all activations can be found in Appendix B.5.

(a) Before ignition **(b)** Beginning of first activation

Figure 4.19: Honda Civic GL before ignition and right after the first deluge activation

4.7.2 Timeline of Events

First activation

The first activation of the deluge system occurred when the fire had a mean flame height of 1.71m. The corresponding HRR of 0.88 MW underwent a deluge activation of 4.7 mm/min during 100 seconds. The temperatures in the immediate vicinity of the car kept rising slightly.

Second activation

The deluge system was activated a second time with 8.6 mm/min on a fire with mean flame height of 2.49m and equivalent 1.45 MW heat release rate. The deluge system remained active for 100 seconds. As a result of the deluge activation, all temperatures around the car gradually dropped whereas the temperature inside the car slightly rose.

Third activation

The third deluge activation of 14.1 mm/min was activated when the mean flame height was 1.49m (0.75 MW). This water flow made the temperatures above the car drop instantly. The temperatures right next to the car rose

before dropping instantly as well. Similarly to the second activation of test 2, this is likely to be linked to the steam initially pushing the flame down.

4.7.3 Measurements

Figure 4.20 shows that 4.7 mm/min of the first activation manages to stabilise the temperatures around the car. Between activation and deactivation, the temperatures of all five thermocouples in table 4.7 rose. However, the temperature rise for the thermocouples right above the roof is only 6-12°C and next to the car the rise in temperature is only 21-35°C. The temperature rise of almost 700°C underneath the roof suggests that the fire grew significantly but is successfully contained inside the car. Figure 4.21a shows the rise in temperature of the centre and side thermocouple tree as a function of height.

It can be seen from figure 4.20 that, for the second activation, the growth is halted and a downward trend occurs. Halfway during the 100-second sprinkler activation, the temperatures next to the car make a significant drop from just under 300°C to about 70°C. The temperature at 2.5 m height (T4) undergoes a similar drop right before sprinkler deactivation. From figure 4.20 it can be seen that the temperature right above the car at 1.75 m (T5) makes a similar drop after the water spray was stopped. However, at the time of sprinkler deactivation this temperature had only dropped from 531°C to 366°C. Figure 4.21b shows how the side temperatures get cooled below 70°C along the height of the test setup. It also shows that, apart from the temperature right above the car, the centre temperatures drop below 125°C. As mentioned earlier, right after sprinkler deactivation, the temperature right above the car makes a big drop.

During the third activation on a fire of 0.75 MW, the highest water flow of 14.1 mm/min was used. Consequently, a big drop in temperatures all around the car occurs. In this case, even the temperature under the roof drops 737°C from 864°C to 127°C. Figure 4.20 shows that the drop in temperature occurred instantly above the car, whereas it takes up to about 75 seconds for the temperature right next to the car to drop instantly. The drop in temperature underneath the roof occurred throughout the sprinkler activation. The temperature profiles for this test is shown in figure 4.21c.

The fourth, fifth and sixth sprinkler activations are very similar (see Appendix B.5). All these sprinkler activations managed to drop the temperatures around the car to about ambient (35°C), analogous to the figure 4.21d.

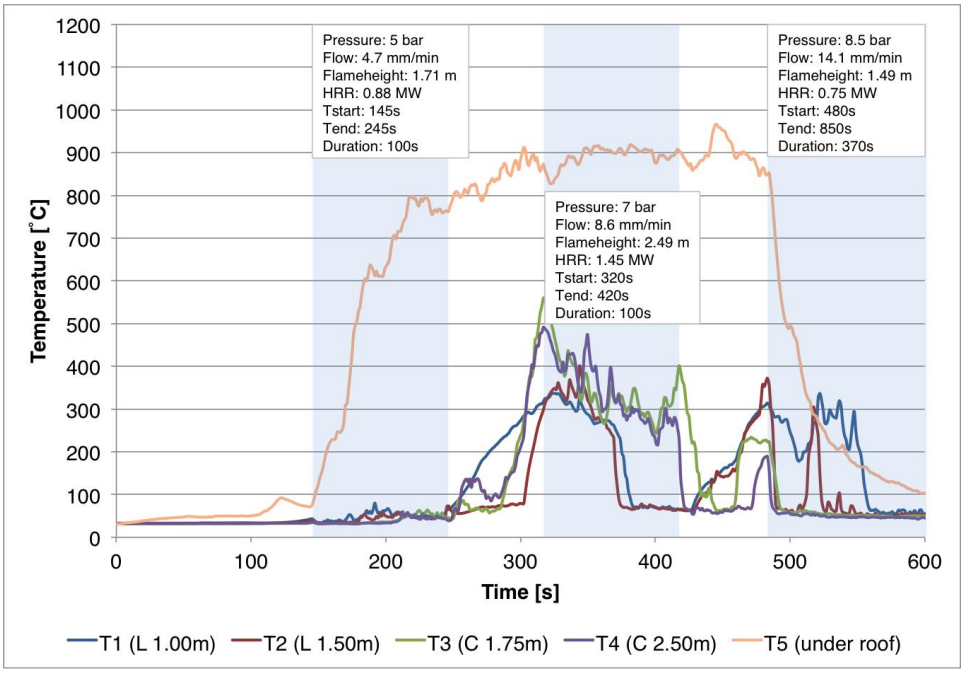

Figure 4.20: Temperature-time curves for the first three sprinkler activations of Test 5 (Full graph in Appendix B.5)

Table 4.7: Impact of the deluge system for Test 5

	Time	T1 [°C]	T2 [°C]	T3 [°C]	T4 [°C]	T5 [°C]
0.88 MW	t_{145}	43	37	35	35	79
4.7 mm/min	t_{245}	64	72	47	41	764
1.45 MW	t_{320}	326	329	531	477	839
8.6 mm/min	t_{420}	65	63	366	101	894
0.75 MW	t_{480}	305	358	226	180	864
14.1 mm/min	t_{580}	64	53	48	46	127
1.11 MW	t_{1260}	49	55	134	243	336
8.6 mm/min	t_{1360}	41	34	34	32	67
0.82 MW	t_{1485}	37	34	81	139	169
6.6 mm/min	t_{1585}	36	34	35	32	63
0.75 MW	t_{2005}	47	33	205	232	327
14.1 mm/min	t_{2105}	35	35	34	33	46
0.52 MW	t_{2340}	34	29	43	53	56
8.6 mm/min	t_{2440}	35	33	34	32	36

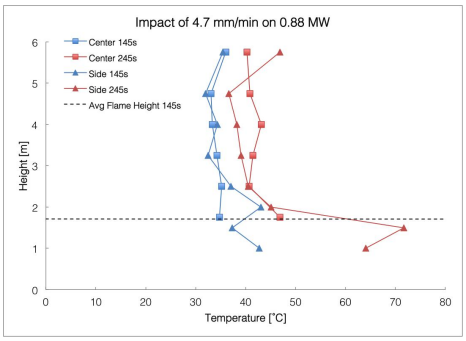

(a) Test 5.1

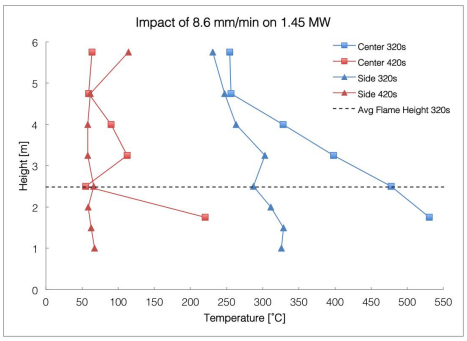

(b) Test 5.2

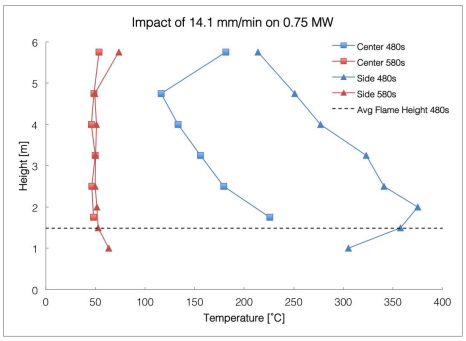

(c) Test 5.3

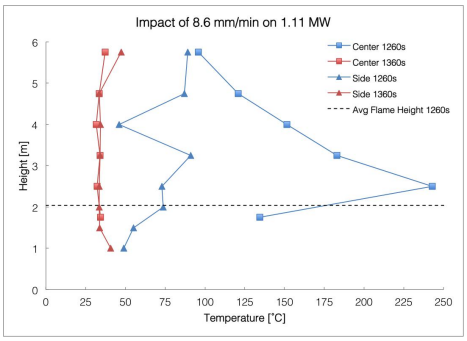

(d) Test 5.4

Figure 4.21: Temperature profiles for Test 5 (Full list in Appendix C.2)

Chapter 5

Analysis and Discussion

As an initial attempt to categorise the data, the data is divided on whether the temperature dropped or kept rising after sprinkler activation. For this criterion the temperature data at sprinkler activation is compared to the temperature data at deactivation. Figure 5.1a shows the result of this assessment.

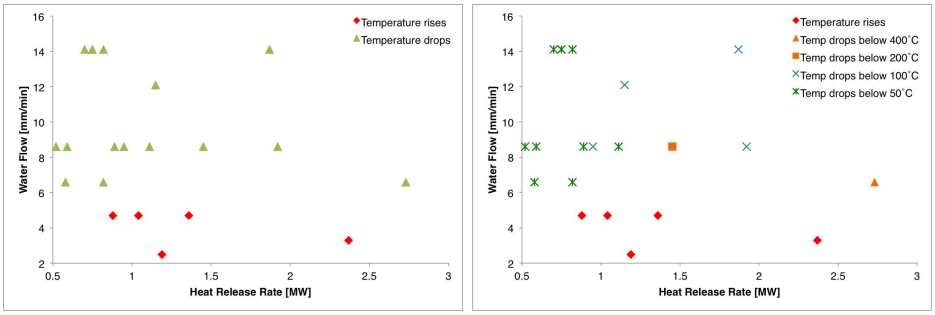

(a) Temperature rise or drop **(b)** Quantified temperature drop

Figure 5.1: Sprinkler effect for all experiments

Rather than expressing the sprinkler performance from a success/failure point of view, a more quantifiable approach is required. In order to achieve this, the temperature drops in figure 5.1a are divided in several discrete intervals. The actual thresholds that are defined are linked with the systems' objective. If it is desired to drop the temperatures to below flaming temperatures, 400°C can be used as a threshold [26]. If the sprinkler system is to eliminate the potential for pyrolysis, 200°C can be used a threshold. This is the temperature at which wood will start pyrolysing [6]. The second most conservative threshold set forward is a temperature drop to below 100°C and, finally, a drop to below 50°C is defined as practically bringing down the temperatures to ambient. Figure 5.1a shows the different sprinkler activations divided according to these suppression criteria. In essence, this

figure shows the capability to drop the temperatures around a burning car during 100 seconds of deluge activation.

It is important to note that the data points from 5.1a are derived from activating the sprinkler system for 100 seconds. Hence, dividing the data in these distinct suppression categories is very dependent on the experimental duration. For instance, the 'Temperature drop below 200°C' data point is the second activation from test 5. Figure 4.20 clearly shows a downward trend in the temperature. This drop in temperature is expected to have continued to below 100°C if the sprinkler system was activated for a longer time.

A more comprehensive suppression-effect classification is applied in the following section. A drop in temperature during the 100 seconds of sprinkler activation is divided in three main categories: a gradual drop in temperatures, an instant drop in temperatures and a temperature rise after deluge activation. The former scenario is a drop that occurs steadily when the system is active. 'An instant drop' is the scenario where the temperature drops to below 100°C within 20 seconds of sprinkler activation. This category is subdivided to include the effect of the steam pushing down the flame and making the temperature right next to the car rise before dropping instantly as well. Basically this effect delays the instant drop right next to the car. Lastly, there is the scenario where the temperature continues to rise. Figure 5.2 is the result of applying this classification on the experimental results.

The data points corresponding to the three main categories appear to correlate with as many regions in figure 5.2. However, the number of data points is insufficient to categorise the plot in three distinct regions. The transition from one sprinkler effect to another is therefore marked with shaded regions. The most conservative approach to these shaded areas is to assume that the 'worst' scenario would occur in this particular region i.e. a temperature rise in the horizontal shaded bar and a gradual rise in the diagonal region. The thresholds between these three regions cannot be determined more accurately than the shaded areas from the given set of data.

It is found that above 6.6 mm/min, the water flow is expected to drop the temperatures around a burning car. Whether this drop in temperature is instantaneous or gradual, depends on the water flow that is applied. Essentially, there are two ways of achieving an instant drop in temperature: one is to increase the water flow, another is to keep the fire size small enough. The latter basically comes down to minimising the activation time.

In the previous discussion, the temperatures around the car were assessed and led to a division of possible sprinkler effects. This is highly relevant for tunnel fire safety design; if one is to design a deluge system for a tunnel

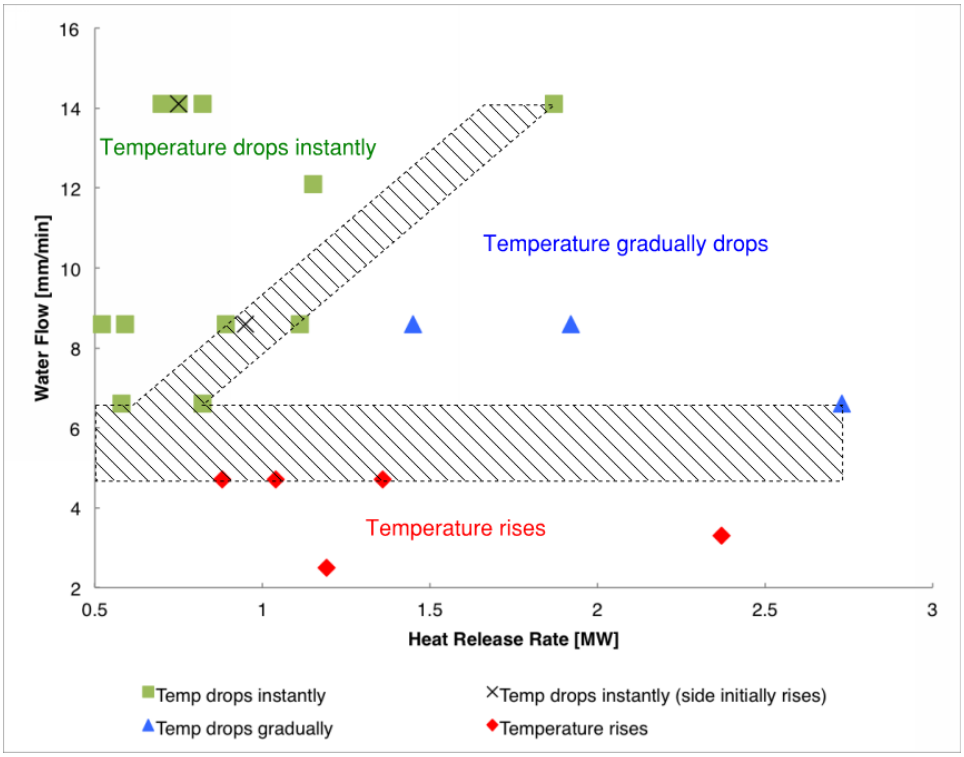

Figure 5.2: Sprinkler effect on the temperatures in the immediate vicinity of a car fire

with a very high expected traffic density, eliminating the potential for fire spread basically comes down to dropping the temperatures in the immediate vicinity of the car. However, if the expected tunnel traffic density is not that high and the vehicle lanes are not particularly narrow, the fire spread to adjacent cars might be less relevant. In that case, one could design for keeping temperatures at the tunnel interface below a certain threshold. Designing for this criteria is likely to be less strict compared to what is presented in figure 5.2.

Chapter 6

Conclusion

A series of full-scale fire tests were conducted in order to assess the required deluge sprinkler water flow for suppression of car fires. Three suppression regimes were identified: one where you have an instant drop in temperatures around the car, another where this drop occurs gradually; and lastly the scenario where the fire is not controlled and the temperatures keep rising. In some cases where instantaneous suppression occurred, the temperature right next to the car rose before eventually dropping sharply as well. This effect is likely to be linked with the steam pushing down the flame from above.

It was found that there are two ways of achieving an instantaneous drop in temperature. One is to apply a sufficiently high water flow, another is to have a smaller fire size. The former would lead to a more conservative, expensive system whereas the latter basically comes down to minimising the activation time. This emphasises the importance of rapid deluge activation.

The boundaries between the three regimes depend on the flow of water that is applied. It was shown that 6.6 mm/min managed to drop the temperatures around a burning car. Below this water flow the fire is assumed to be out of control. It must be noted that these results are only valid for the exact configuration as tested, with no ventilation and for the given fire sizes.

Whether an instant or a gradual drop in temperature is required, depends on the distance to an adjacent car. This directly relates to the expected traffic density and car lane width. The results presented in this thesis can help in the design of deluge sprinkler systems in tunnels.

Future research must investigate the effects of the potential rise in temperature right next to the car following deluge activation. The thresholds between the different suppression regimes must be narrowed down by performing similar tests.

Additional analysis on scalability is required to investigate applicability on heavy goods vehicles. Lastly, the influence of droplet size and longitudinal ventilation must be looked into.

Bibliography

[1] 499, E. Fires in transport tunnels: Report on full-scale test eureka-project eu499:. Tech. Rep. D-40213, FIRETUN Studiensgesellschaft Stahlanwendung e.V., Dusseldorf, 1995.

[2] Agnew, N., and Allen, B. Full scale car burns in the Sydney Harbour Tunnel. *Fire Australia 2008* (2008).

[3] Babrauskas, V. *SFPE Handbook of Fire Protection Engineering*, fifth edition ed., vol. 1. Springer, 2016, ch. Heat Release Rates, p. 891.

[4] Bilson, M., Purchase, A., and Stacey, C. Deluge system operating effectiveness in road tunnels and impacts on operating policy. In *13th Australian Tunnelling Conference Proceedings* (Melbourne, May 2008).

[5] Brousse, B., and Lacroix, D. Technical report - part 2 fire safe design. Tech. rep., Thematic Network FIT - Fire in Tunnels, 2006.

[6] Buchanan, A. H. *Structural Design for Fire Safety.* Wiley, 2002, ch. 10 Timber Structures, p. 277.

[7] Carvel, R. Design fires for tunnel water mist suppression systems. In *Proc. 3rd Int Symp. On Tunnel Safety and Security* (Stockholm, Sweden, March 2008), pp. 141–148.

[8] Carvel, R. Mitigation of tunnel fires. In *Proceedings from the Fifth International Symposium on Tunnel Safety and Security (ISTSS 2012)* (March 2012).

[9] Carvel, R., and Ingason, H. *SFPE Handbook of Fire Protection Engineering*, fifth edition ed., vol. 3. Springer, 2016, ch. Fires in Vehicle Tunnels, pp. 3303–3325.

[10] Congress, P. X. W. Reports by technical committees. Tech. rep., THE WORLD ROAD ASSOCIATION (PIARC), 1987.

[11] Council, E. *Directive 2004/54/EC of the European Parliament and of the Council of 29 April 2004 on minimum safety requirements for tunnels in the Trans-European Road Network.*

[12] Dessel, J. V., and Martin, Y. General report. Tech. rep., Thematic Network FIT - Fire in Tunnels, 2006.

[13] FMRC. *Loss Prevention Data, Storage of plastics and elastomers including polyurethane, expanded rubber and crude natural and crude synthetic rubber.* Factory Mutual System, February 1981.

[14] Guillermo Rein, Ricky Carvel, J. L. T. Approximate trajectories of droplets from water mist suppression systems in tunnels. In *Proceedings from the Third International Symposium on Tunnel Safety and Security* (Stockholm, Sweden, September 2008), BRE Centre for Fire Safety Engineering.

[15] Haack, A. Technical report - part 1 design fire scenarios. Tech. rep., Thematic Network FIT - Fire in Tunnels, 2006.

[16] Haack, A., Schreyer, J., Meyeroltmanns, W., and Beyer, S. Brandschutz in verkehrstunnels. Tech. rep., BASt - Bundesanstalt für Strassenwesen, Köln, December 2000.

[17] Harris, K. J. Water application rates for fixed fire fighting systems in road tunnels. In *Proceedings from the Fourth International Symposium on Tunnel Safety and Security* (Frankfurt am Main, Germany, March 2010), SP Technical Research Institute.

[18] Heskestad, G. *SFPE Handbook of Fire Protection Engineering*, fifth edition ed., vol. 1. Springer, 2016, ch. Fire Plumes, Flame Height, and Air Entrainment, p. 402.

[19] Höj, N. P. Technical report - part 2 fire safe design - road tunnels. Tech. rep., Thematic Network FIT - Fire in Tunnels, 2006.

[20] Ingason, H. *Flammability testing of materials used in construction, transport and mining.* Woodhead Publishing, 2006, ch. Fire Testing in Road and Railway Tunnels, pp. 231–274.

[21] Ingason, H., Bergqvist, A., Lönnermark, A., Frantzich, H., and Hasselrot, K. Räddningsinsatser i vägtunnlar. Tech. rep., Räddningsverket, 2005.

[22] Ingason, H., et al. *Tunnel Fire Dynamics.* Springer Science, 2015.

[23] Ingason, H., Gustavsson, S., and Werling, P. Brandförsök i en bergtunnel - naturlig ventilation delrapport ii. Tech. Rep. SP AR

1995:45, SP Technical Research Institute of Sweden, Borås, Sweden, 1995.

[24] Joyeux, D. Natural fires in closed car parks - car fire tests. Tech. Rep. INC 96/294d DJ/NB, CTICM, Metz, France, 1997.

[25] Lacroix, D. New french recommendations for fire ventilation in road tunnels. In *9th International Conference on Aerodynamics and Ventilation of Vehicle Tunnels* (Aosta Valley, October 1997).

[26] Lindström, B., Karlsson, J. A. J., Ekdunge, P., Verdier, L. D., Häggendal, B., Dawody, J., Nilsson, M., and Pettersson, L. J. Diesel fuel reformer for automotive fuel cell applications. *International Journal of Hydrogen Energy* (2009).

[27] Lönnermark, A. *On the Characteristics of Fires in Tunnels*. PhD thesis, Lund University, Lund, Sweden, 2005.

[28] Lönnermark, A., Lindström, J., Li, Z.Y., Ingason, H., and Kumm, M. Large-scale commuter train tests - results from the metro project. In *Proceedings from the Fifth International Symposium on Tunnel Safety and Security (ISTSS 2012)* (New York, USA, March 2012), pp. 447–456.

[29] Mangs, J., and Keski-Rahkonen, O. Characterization of the fire behaviour of a burning passenger car. part i: Car fire experiments. *Fire Safety Journal 23* (1994), 17–35.

[30] McCaffrey, J. B. Some measurements of the radiative power output of diffusion flames. Tech. Rep. Paper WSS/CI81-15, Western States Meeting of Combustion Institute, Pullman, Washington, 1981.

[31] NFPA 13. *Standard for the Installation of Sprinkler Systems*, 2013 edition ed. Batterymarch Park, Quincy, MA 02169-7471, 2013.

[32] NFPA 502. *Standard for Road Tunnels, Bridges and other limited Access Highways*. Batterymarch Park, Quincy, MA 02169-7471, 2001.

[33] Persson, H. Commodity classification - a more objective and applicable methodology. Tech. Rep. 70, SP Technical Research Institute of Sweden, 1993.

[34] PIARC. Road tunnels technical committee 5 report. Tech. rep., THE WORLD ROAD ASSOCIATION (PIARC), 1999.

[35] PIARC. Road tunnels: An assessment of fixed fire fighting systems. Tech. rep., THE WORLD ROAD ASSOCIATION (PIARC), 2008.

[36] PIARC. Fixed fire fighting systems in road tunnels: Current practices and recommendations. Tech. rep., THE WORLD ROAD ASSOCIATION (PIARC), 2016.

[37] Quintiere, J. G. Scaling applications in fire research. *Fire Safety Journal* (1989).

[38] Rew, C., and Deaves, D. Fire spread and flame length in ventilated tunnels - a model used in channel tunnel assessments. In *Proceedings of the International Conference on Tunnel Fires and Escape from Tunnels* (Lyon, France, May 1999), Independent Technical Conferences Ltd, pp. 397–406.

[39] Rhodes, N., and MacDonald, M. Technical report - part 3 fire safe design. Tech. rep., Thematic Network FIT - Fire in Tunnels, 2006.

[40] RUS120:3. *Regler för automatisk vattensprinkleranläggning.* FSAB Fösäkringsbranschens Serviceaktiebolag, 1993.

[41] Sheppard, D. T. *Spray Characteristics of Fire Sprinklers.* PhD thesis, Northwestern University, 2002.

[42] Shipp, M., and Spearpoint, M. Measurements of the severity of fires involving private motor vehicles. *Fire and Materials 19* (May/June 1995), 143–151.

[43] SOLIT2. *Engineering Guidance for a Comprehensive Evaluation of Tunnels With Fixed Fire Fighting Systems.* SOLIT2 Project, 2012.

[44] Steinert, C. Experimentelle untersuchhungen zum abbrand und feuerubersprungsverhalten van personenkraftwagen. *FVDB-Zeitschrift*, 4 (2000), 63–172.

[45] Stroeks, R. Sprinklers in japanese road tunnels. Tech. rep., Ministry of Transport, The Netherlands, 2001.

[46] Wu, Y., and Carvel, R. *Handbook of Tunnel Fire Safety*, 2nd edition ed. ICE Publishing, 2011, ch. 8 Water-based fire-suppression systems for tunnels, pp. 127–149.

[47] Xin, Y., and Tamanini, F. Assessment of commodity classification for sprinkler protection using representative fuels. In *Fire Safety Science-Proceedings of the Ninth International Symposium* (2008), International Association for Fire Safety Science, pp. 527–538.

[48] Yao, C. Overview of fmrc's sprinkler technology research. In *First International Conference on Fire Suppression Research* (1992), Factory Mutual Research Corporation, NIST.

Appendix A

Water Distributions

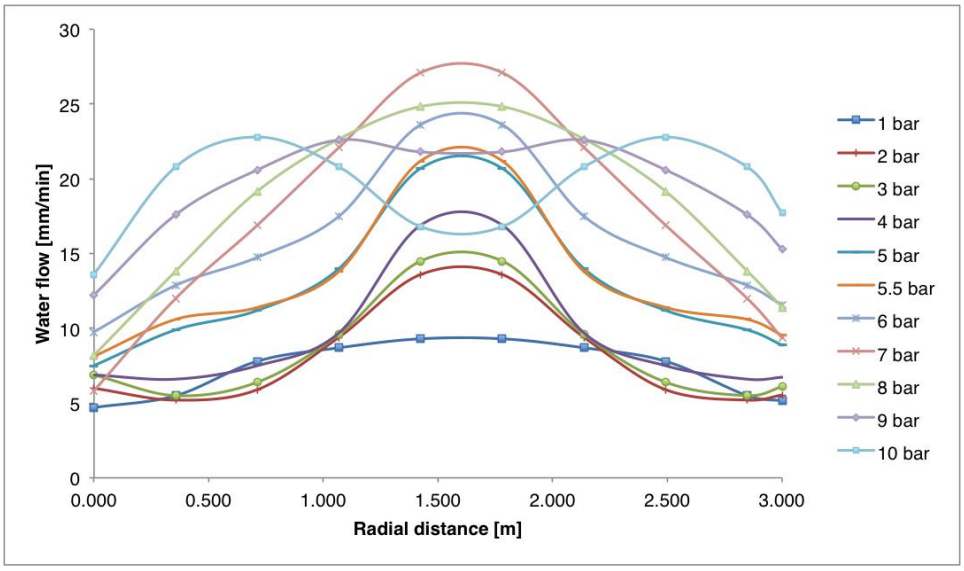

Figure A.1: Water distribution for a nozzle spacing of 3m

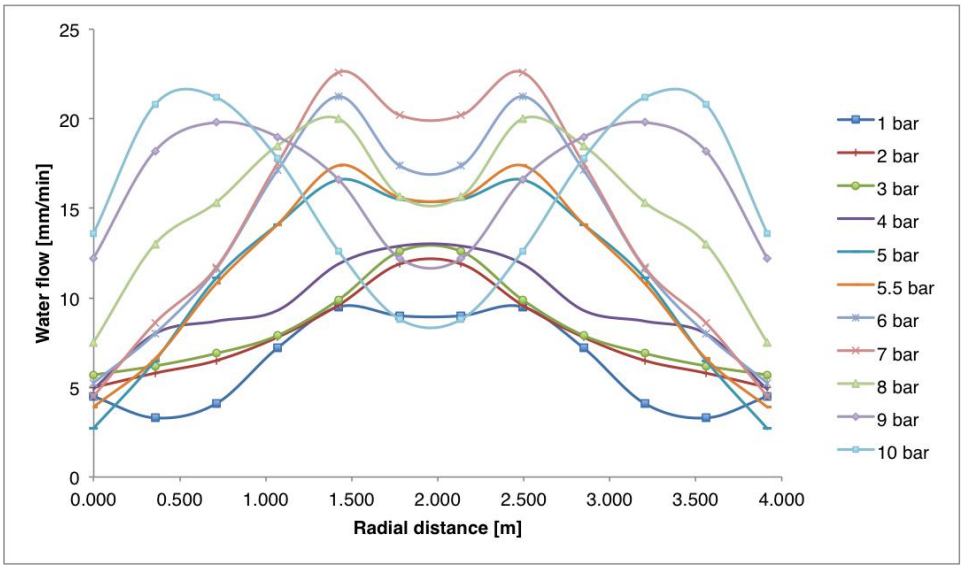

Figure A.2: Water distribution for a nozzle spacing of 4m

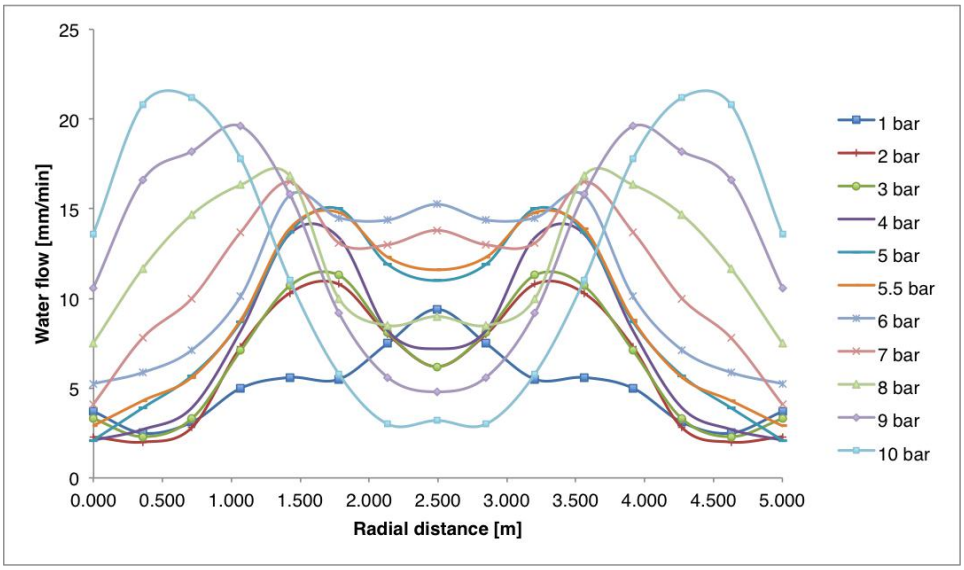

Figure A.3: Water distribution for a nozzle spacing of 5m

Appendix B

Thermocouple Data

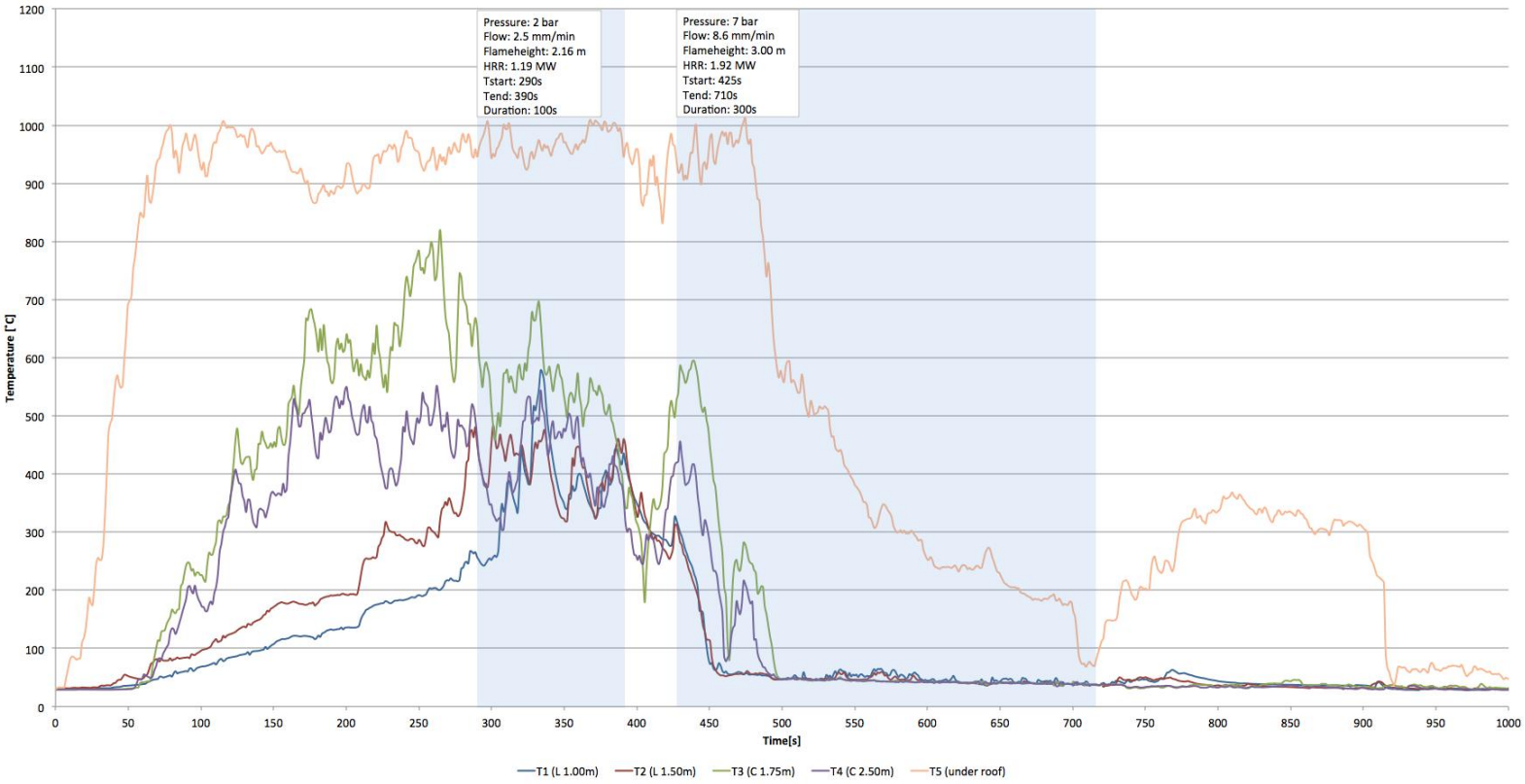

Figure B.1: Temperature data Test 1

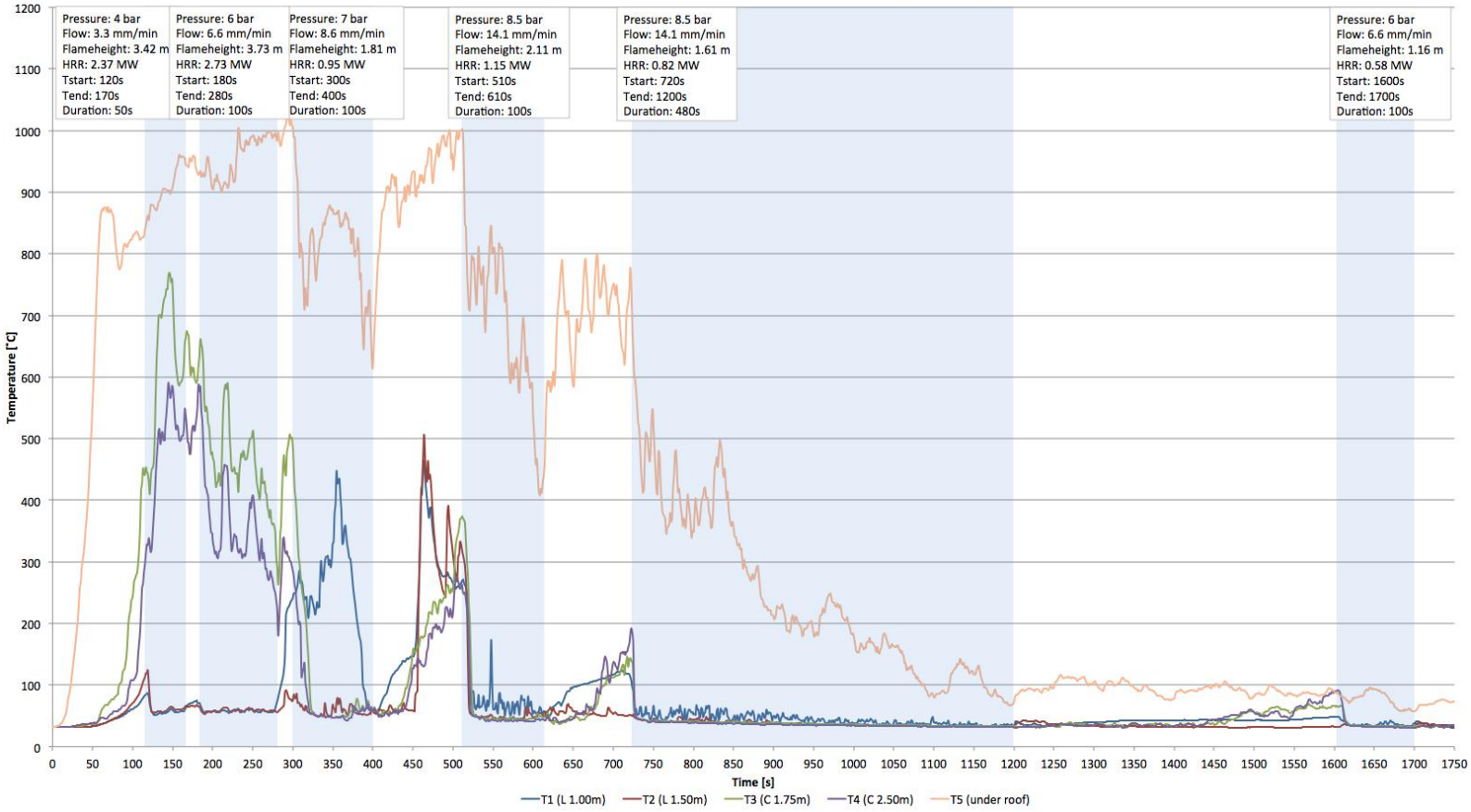

Figure B.2: Temperature data Test 2

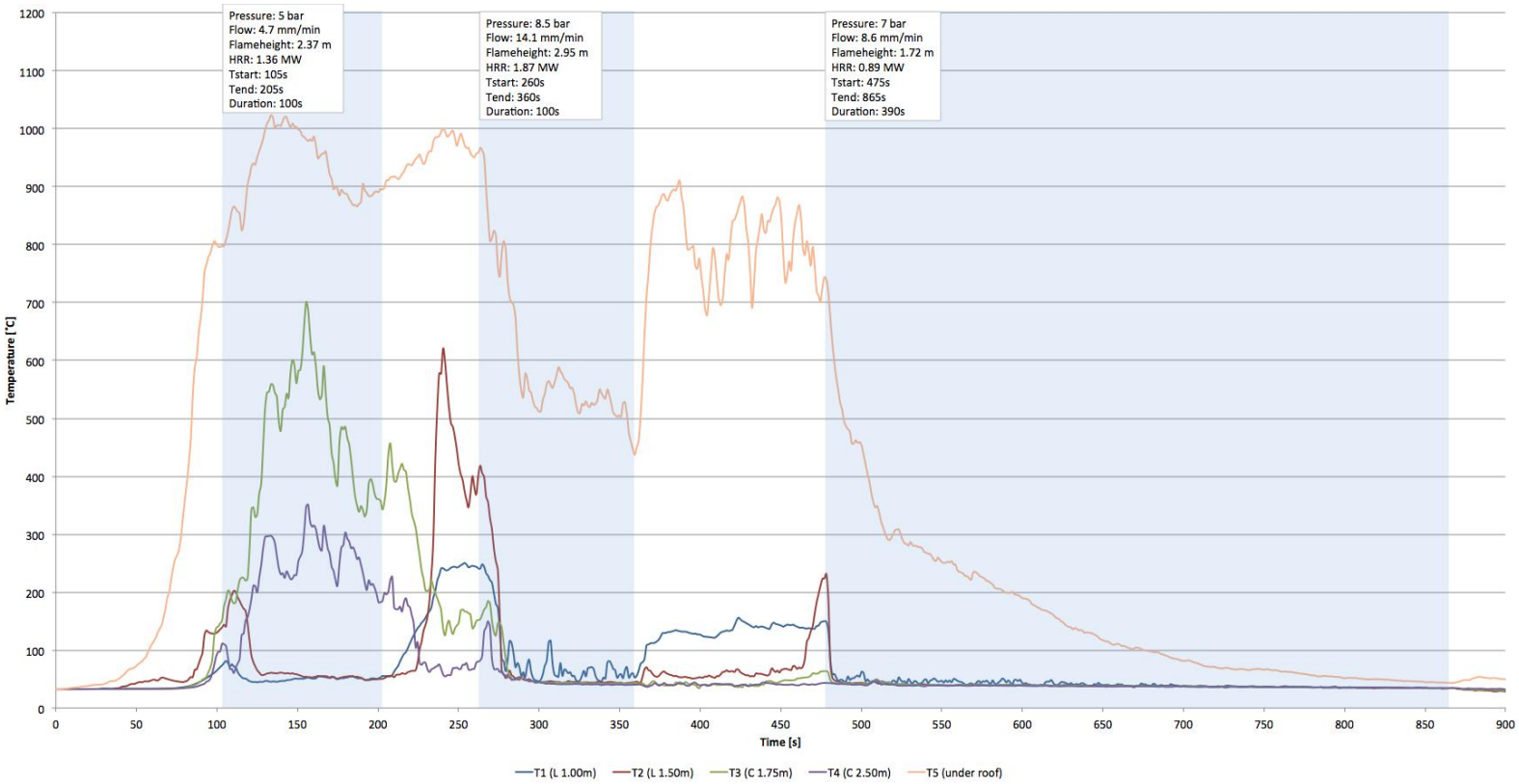

Figure B.3: Temperature data Test 3

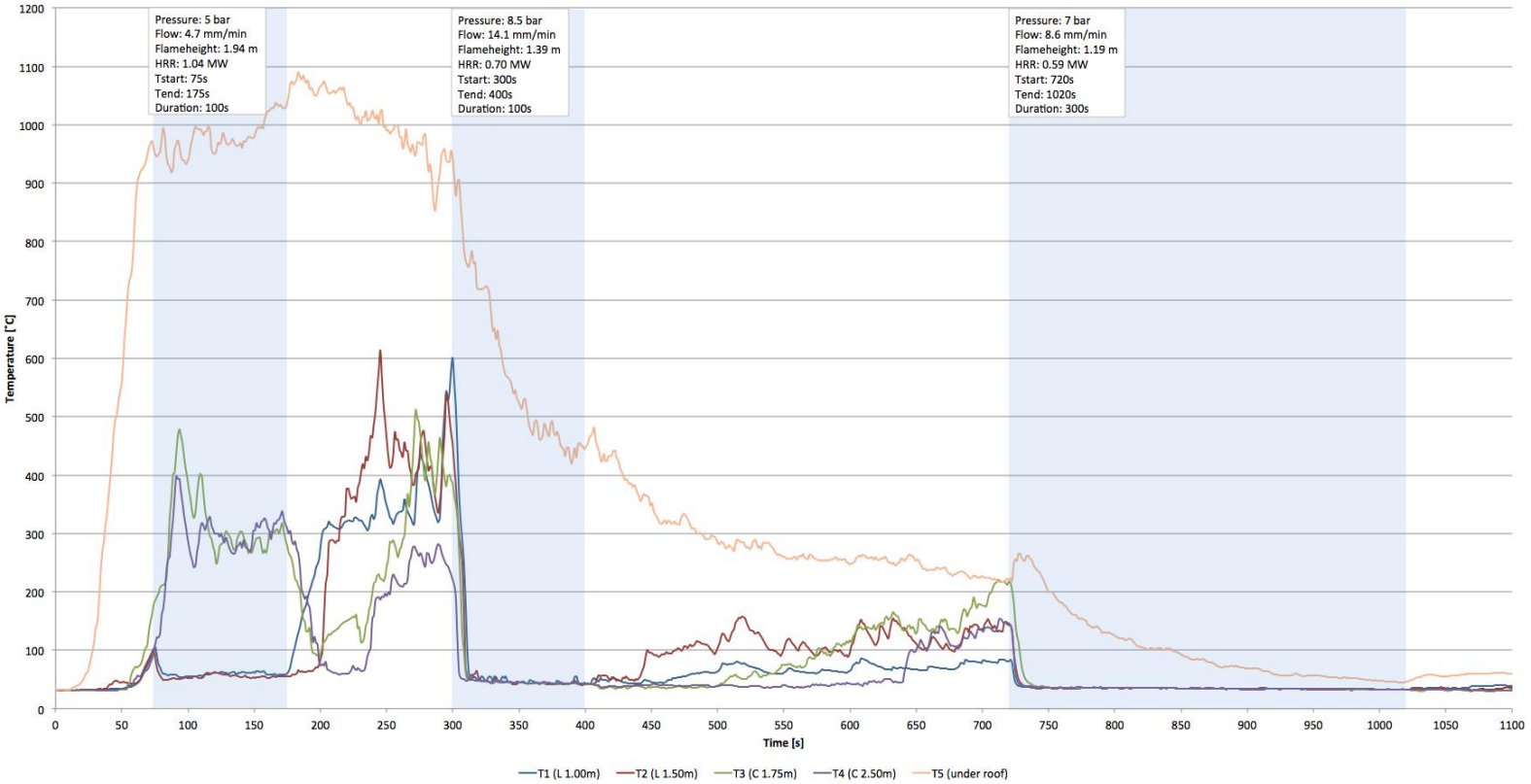

Figure B.4: Temperature data Test 4

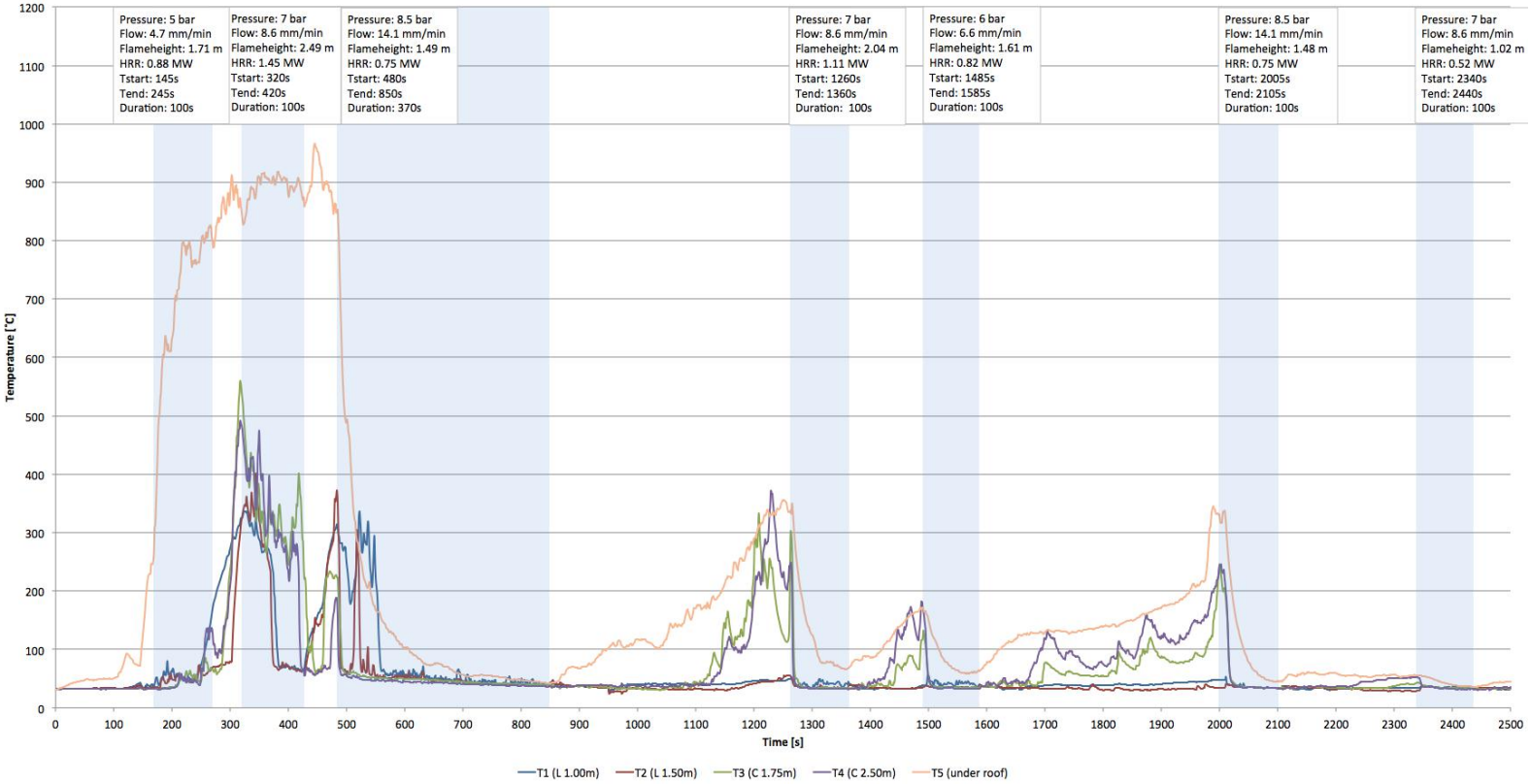

Figure B.5: Temperature data Test 5

Appendix C

Impact of Sprinkler on Temperature

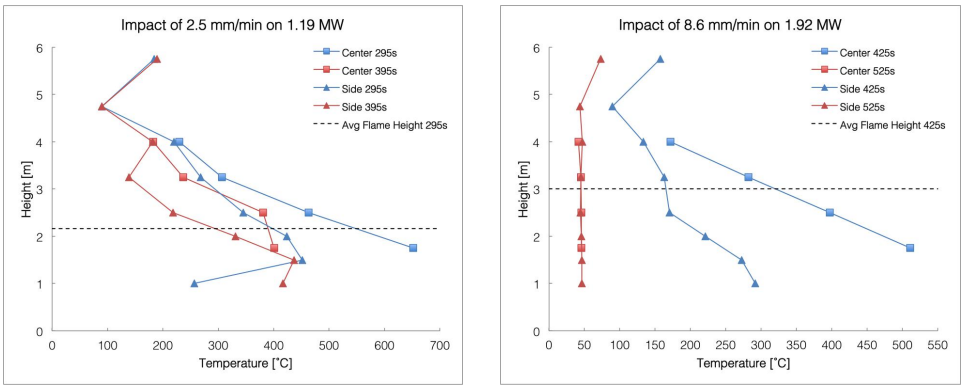

(a) Test 1.1 **(b)** Test 1.2

Figure C.1: Temperature profiles for Test 1

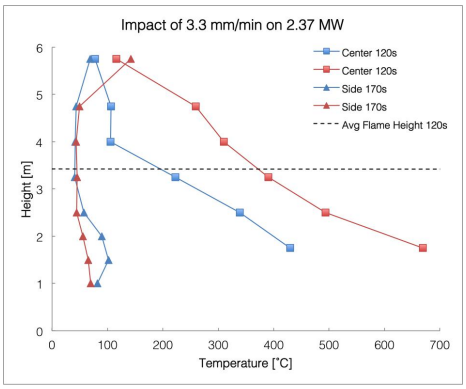

(a) Test 2.1

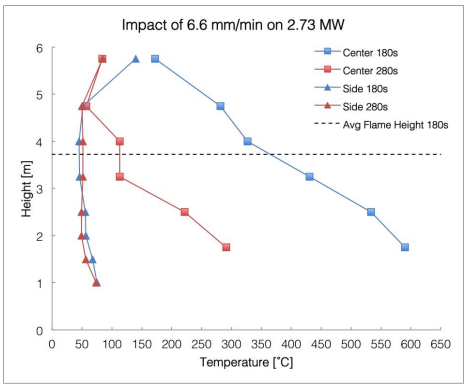

(b) Test 2.2

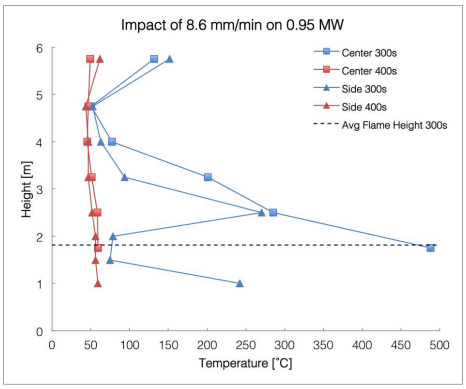

(c) Test 2.3

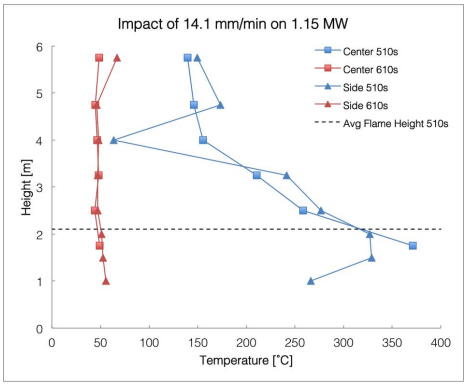

(d) Test 2.4

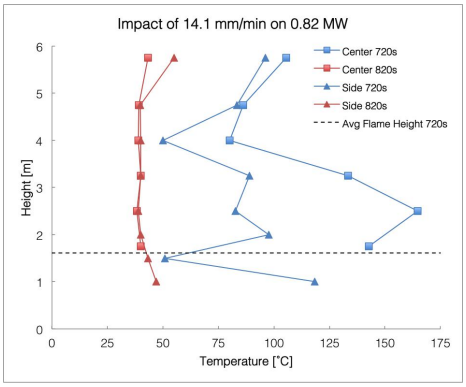

(e) Test 2.5

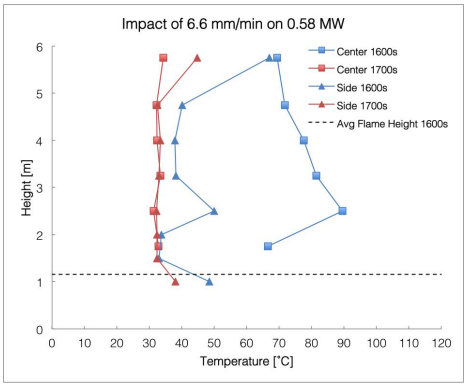

(f) Test 2.6

Figure C.2: Temperature profiles for Test 2

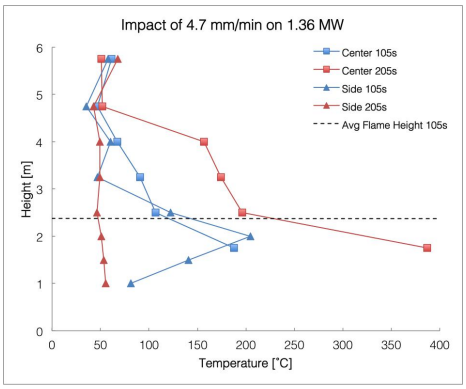

(a) Test 3.1

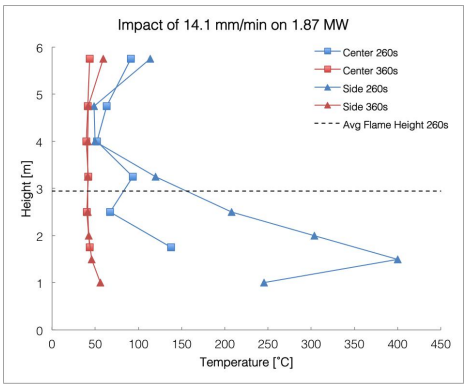

(b) Test 3.2

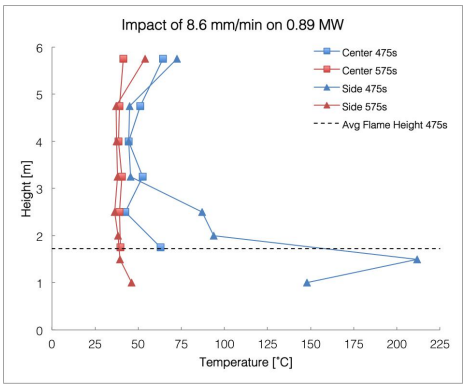

(c) Test 3.3

Figure C.3: Temperature profiles for Test 3

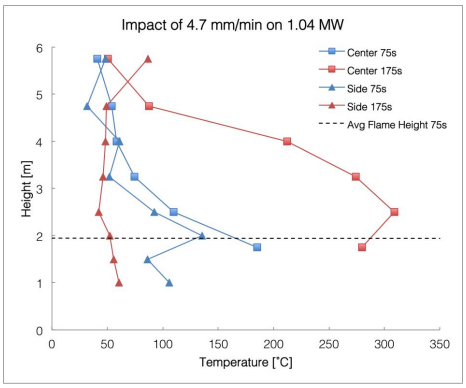

(a) Test 4.1

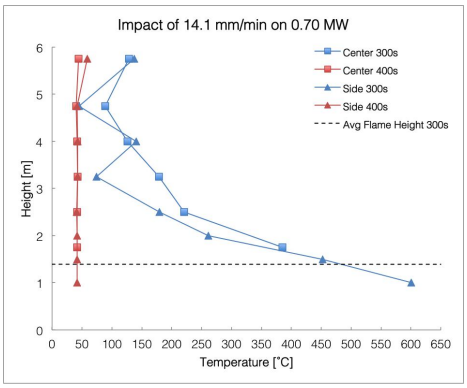

(b) Test 4.2

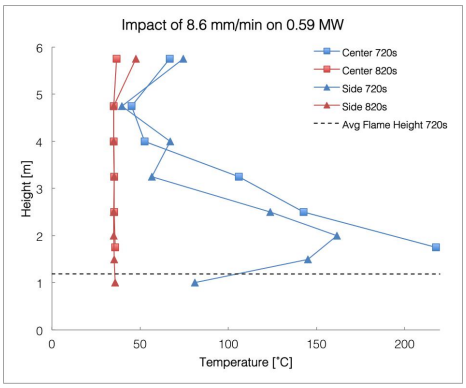

(c) Test 4.3

Figure C.4: Temperature profiles for Test 4

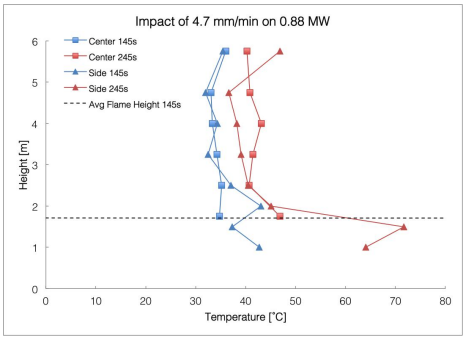

(a) Test 5.1

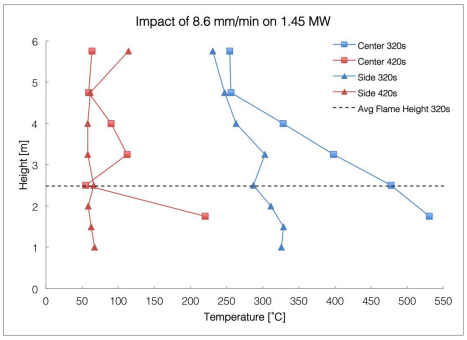

(b) Test 5.2

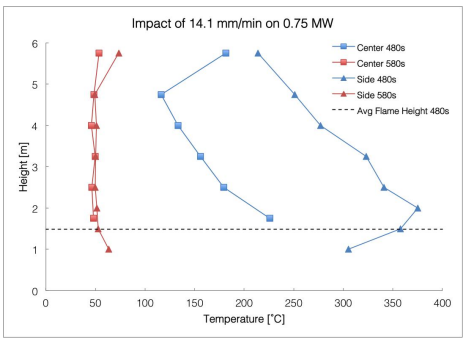

(c) Test 5.3

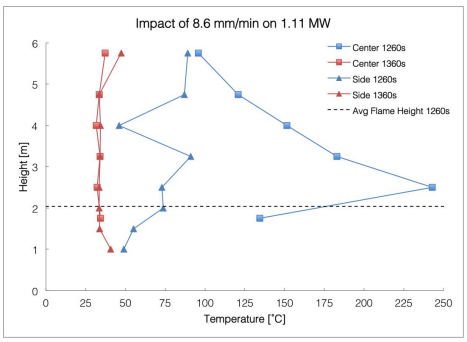

(d) Test 5.4

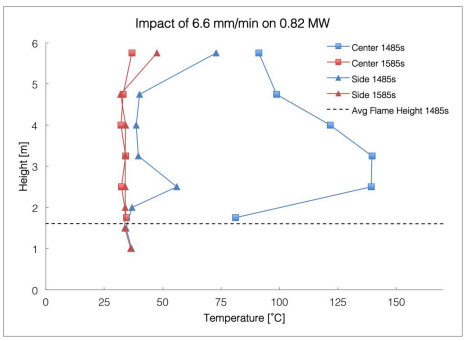

(e) Test 5.5

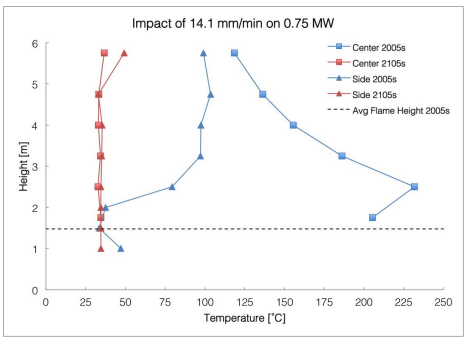

(f) Test 5.6

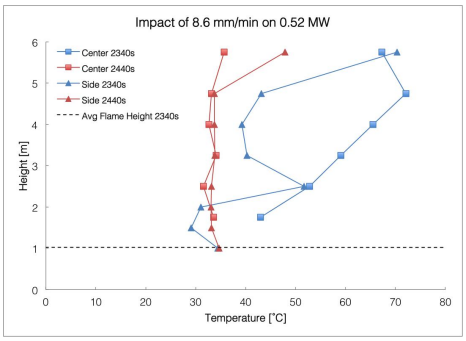

(g) Test 5.7

Figure C.5: Temperature profiles for Test 5